JOINT TRANSPORTATION
RESEARCH PROGRAM
INDIANA DEPARTMENT OF TRANSPORTATION
AND PURDUE UNIVERSITY

Determining Asphalt Mixture Properties Using Imaging Techniques

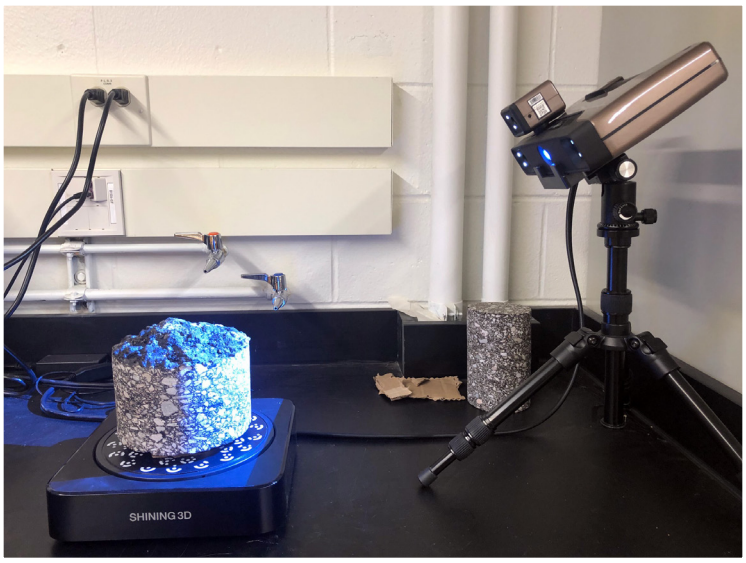

Mohammad Ali Notani, Behnam Jahangiri,
Reyhaneh Rahbar Rastegar, John E. Haddock

SPR-4415 • Report Number: FHWA/IN/JTRP-2023/12 • DOI: 10.5703/1288284317635

RECOMMENDED CITATION

Notani, M. A., Jahangiri, B., Rastegar, R. R., & Haddock, J. E. (2023). *Determining asphalt mixture properties using imaging techniques* (Joint Transportation Research Program Publication No. FHWA/IN/JTRP-2023/12). West Lafayette, IN: Purdue University. https://doi.org/10.5703/1288284317635

AUTHORS

Mohammad Ali Notani
Graduate Research Assistant
Lyles School of Civil Engineering
Purdue University

Behnam Jahangiri, PhD, PE
Lead Research Scholar
Lyles School of Civil Engineering
Purdue University

Reyhaneh Rahbar Rastegar, PhD, PE
Research Engineer
Lyles School of Civil Engineering
Purdue University

John E. Haddock, PhD, PE
Professor of Civil Engineering
Director of the Local Technical Assistance Program
Purdue University
(765) 496-3996
jhaddock@purdue.edu
Corresponding Author

JOINT TRANSPORTATION RESEARCH PROGRAM

The Joint Transportation Research Program serves as a vehicle for INDOT collaboration with higher education institutions and industry in Indiana to facilitate innovation that results in continuous improvement in the planning, design, construction, operation, management and economic efficiency of the Indiana transportation infrastructure. https://engineering.purdue.edu/JTRP/index_html

Published reports of the Joint Transportation Research Program are available at http://docs.lib.purdue.edu/jtrp/.

NOTICE

TECHNICAL REPORT DOCUMENTATION PAGE

1. Report No. FHWA/IN/JTRP-2023/12	**2. Government Accession No.**	**3. Recipient's Catalog No.**
4. Title and Subtitle Determining Asphalt Mixture Properties Using Imaging Techniques		**5. Report Date** April 2023 **6. Performing Organization Code**
7. Author(s) Mohammad Ali Notani, Behnam Jahangiri, Reyhaneh Rahbar Rastegar, and John E. Haddock		**8. Performing Organization Report No.** FHWA/IN/JTRP-2023/12
9. Performing Organization Name and Address Joint Transportation Research Program Hall for Discovery and Learning Research (DLR), Suite 204 207 S. Martin Jischke Drive West Lafayette, IN 47907		**10. Work Unit No.** **11. Contract or Grant No.** SPR-4415
12. Sponsoring Agency Name and Address Indiana Department of Transportation (SPR) State Office Building 100 North Senate Avenue Indianapolis, IN 46204		**13. Type of Report and Period Covered** Final Report **14. Sponsoring Agency Code**

15. Supplementary Notes

Conducted in cooperation with the U.S. Department of Transportation, Federal Highway Administration.

16. Abstract

This study introduces imaging technology to determine the bulk specific gravity (G_{mb}) of compacted asphalt mixture specimens. Using an advanced three-dimensional scanner, a fast, accurate technique for determining compacted asphalt mixture specimen G_{mb} was developed. The feasibility of this technique was evaluated by testing a collection of asphalt mixtures, including dense-graded and stone mastic asphalt mixtures. The results were compared with those obtained using the currently-specified G_{mb} measurement methods of AASHTO T166 and CoreLok. The proposed scanning technique was also used for both laboratory-prepared and field-cored specimens to determine its reliability and reproducibility. The study results suggest the proposed imaging technique is effective in decreasing G_{mb} measurement variation as well as in improving the accuracy and reproducibility. Additionally, the results indicate the proposed technique can be applied to any asphalt specimen, regardless of mixture type, aggregate sizes, or fabrication technique.

17. Key Words imaging technique, bulk specific gravity, AASHTO-T166, CoreLok, scanner, asphalt mixture	**18. Distribution Statement** No restrictions. This document is available through the National Technical Information Service, Springfield, VA 22161.

19. Security Classif. (of this report) Unclassified	**20. Security Classif. (of this page)** Unclassified	**21. No. of Pages** 34	**22. Price**

EXECUTIVE SUMMARY

Introduction

The current techniques used to determine the volumetric properties of asphalt mixtures have changed little since their initial adoption. However, with today's technologies, it should be possible to accurately measure materials properties in real-time. Bulk specific gravity (G_{mb}) is one important measurement that must be made on compacted asphalt mixture specimens to determine the volumetric properties of asphalt mixture. Air voids content (V_a), voids in the mineral aggregate (VMA), and voids filled with the asphalt (VFA) are three important volumetric properties used to control the manufacture and performance of asphalt mixtures.

Current conventional methods for determining compacted asphalt mixture specimen G_{mb}, AASHTO T166 and vacuum sealing (CoreLok), are somewhat limited and subject to some restrictions. For example, T166 should not be used with compacted specimens that absorb more than 2% water. The CoreLok method can often experience difficulties when used with mixture specimens that make use of larger aggregate sizes, or specimens that may have rougher exteriors. Using imaging technology to determine the G_{mb} of compacted asphalt mixture specimens can result in better characterization of the mixtures through a higher degree of measurement accuracy than can be done with current techniques.

The main objective of this study is to provide a method that accurately measures the volume, and thus the G_{mb}, of compacted asphalt mixture specimens using a 3-dimensional scanner. To this aim, the project objectives were threefold—(1) develop a testing procedures and testing condition for compacted asphalt specimens, (2) complete a parametric study to determine the optimum values of input parameters, and (3) evaluate the capability of the scanner to measure G_{mb} through a comparative analysis with current standard methods.

Findings

This study recommends a potential imaging method to measure the compacted asphalt specimen G_{mb} accurately and efficiently, thus eliminating the limitations and disadvantages associated with current standard methods. The following are the key findings drawn from this research study.

- Imaging techniques can be a reliable alternative for measuring the G_{mb} of any type of asphalt mixture specimen and can do so more quickly and accurately than current standard methods.
- There is no water absorption limitation with imaging techniques, such as the 2% limit found in AASHTO T166.
- The imaging technique is highly repeatable, when compared to CoreLok and AASHTO T166 methods.
- The accuracy of imaging techniques can eliminate the need for measurement replication.
- The proposed imaging method allows the G_{mb} measurement of asphalt mixture specimens, regardless of mixture type, aggregate size, specimen dimension, and how the specimen is obtained (laboratory produced or field cores).
- The proposed imaging method can produce a highly accurate G_{mb} measurement in 8 minutes or less.
- Measuring asphalt mixture G_{mb} by imaging does not require specific operator expertise, therefore the measurement is independent of the operator skill.

Implementation

The proposed method directly addresses the measurement of compacted asphalt mixture G_{mb} in a relative short time and more accurately than current standard methods. Using the candidate technique will save time and resources when determining asphalt mixture volumetric properties, increase the accuracy of such measurements, and deliver the measurements in real-time.

CONTENTS

LIST OF FIGURES

LIST OF TABLES

1. INTRODUCTION

1.1 Background

There have been continuous enhancements in asphalt mixture design technology to improve the quality of flexible pavements under increasingly heavier loads and traffic volumes (Liu et al., 2022; Montoya et al., 2018; Takahashi & Partl, 2001). These improvements have been achieved using high-quality materials, improved pavement design methods, and careful measurement of volumetric properties as part of the mixture design process. Asphalt mixture design is an important step to ensure asphalt mixture performance. Several factors are considered when designing and testing asphalt mixtures, including the volumetric properties (Dukatz et al., 2009).

Along with laboratory performance testing, asphalt mixture volumetric properties such as binder content (P_b), voids in the mineral aggregates (VMA), voids filled with asphalt (VFA), and air voids content (V_a) have been used to design and evaluate asphalt mixtures. V_a refers to the total amount of air between asphalt-coated aggregate particles as a percentage of the total volume of the compacted HMA specimen and is calculated using Equation 1.1 (Griffith, 2009).

$$V_a = 100 \times \left[1 - \frac{G_{mb}}{G_{mm}}\right] \qquad \text{(Eq. 1.1)}$$

where:

V_a = air voids content (%),
G_{mb} = the bulk specific gravity of the compacted asphalt mixture, and
G_{mm} = the theoretical maximum specific gravity of asphalt mixture.

It is evident from Equation 1.1 that V_a in an asphalt mixture is directly related to the G_{mb} of the mixture. This equation represents the amount of asphalt mixture compaction achieved as compared to the G_{mm}, which is a mixture's specific gravity when the mixture contains no air content.

Voids in the mineral aggregate (VMA) is another volumetric property directly related to the G_{mb} of an asphalt mixture. VMA is the combined volumes of asphalt binder and air in a compacted asphalt mixture. Asphalt mixture VMA can therefore be increased by adding additional binder to a mixture, increasing air voids contents in the mixture, or a combination of both. VMA is calculated using Equation 1.2.

$$VMA = 100 - \left[\frac{G_{mb} \times P_s}{G_{sb}}\right] \qquad \text{(Eq. 1.2)}$$

where:

VMA = voids in the mineral aggregate,
G_{mb} = the bulk specific gravity of the compacted asphalt sample,
P_s = the percent of mineral aggregate in the mixture, and
G_{sb} = the bulk specific gravity of the aggregate blend.

Finally, a third volumetric property often used with asphalt mixtures is the voids filled with asphalt (VFA) (Griffith, 2009). VFA is the proportion of VMA filled with asphalt binder and is calculated as:

$$VFA = 100 \times \left[\frac{VMA \times V_a}{VMA}\right] \qquad \text{(Eq. 1.3)}$$

where:

VFA = voids filled with asphalt binder,
VMA = voids in the mineral aggregate, and
V_a = air voids content.

As is evident in Equation 1.3, if the V_a or VMA of an asphalt mixture changes, the VFA will also change. In fact, the three volumetric properties, V_a, VMA, and VFA, are interrelated such that if any two are fixed, the third volumetric property becomes fixed as well.

The importance of these three volumetric properties in the design and performance of asphalt mixtures cannot be overstated. The Marshall mixture design procedure developed by Bruce Marshall in the late 1930s to early 1940s (ASTM D1559) requires an optimum asphalt binder content to be chosen that results in 3%–5% V_a and meets minimum VMA requirements. Francis Hveem also used V_a to help determine the optimum asphalt binder content in establishing the Hveem mixture design method (ASTM D1560). Most recently, asphalt mixtures designed using the Superpave mixture design method (AASHTO M323) specify optimum binder content be selected at 4% V_a, at a given design number of gyrations (N_{des}). Furthermore, to comply with Superpave requirements, the VMA and VFA parameters need to meet specific conditions. Thus, for these three mixture design methods, two of which are still widely used throughout the world, the resulting asphalt mixture design is heavily dependent on mixture volumetric properties. This highlights the importance of accurately measuring asphalt mixture volumetric properties.

Among these three volumetric properties, V_a has attracted a great deal of attention and is often used as the main criterion for determining optimum asphalt binder content when designing asphalt mixtures. When investigating the importance of V_a, researchers have evaluated the performance of asphalt mixtures produced at different V_a contents (Finn & Epps, 1980; Kassem et al., 2011). Zeiada et al. (2014) showed that changing the V_a of a dense-graded asphalt mixture from 4% to 10% resulted in up to a 50% reduction in dynamic modulus values for the mixture. Harvey and Tsai (1996) demonstrated the benefit of lower V_a through laboratory fatigue and stiffness tests. The fracture toughness (K_f), which indicates cracking resistance potential and is obtained from semi-circular bend (SCB) testing, was improved by up to 25% after reducing the V_a from 7% to 3% (Aliha et al., 2015). Further, Lee et al. (2007) found that by increasing V_a in asphalt mixtures, mixture rutting resistance was

decreased. This was also found to be true in a study conducted by Brown and Cross (1991). Thus, decreasing V_a in asphalt mixtures, to an extent, can improve mixture rutting resistance. Volumetric properties also affect the mechanical performance of asphalt mixtures, with higher V_a making mixtures more prone to cracking (De Freitas et al., 2005; Schwartz et al., 2013; Shen et al., 2016). Therefore, V_a is one of the main asphalt design parameters that can directly affect the mechanical performance of asphalt mixtures.

1.2 Motivation

Asphalt mixture performance is dependent on accurately measuring asphalt mixture volumetric properties, which in turn are dependent on the accurate measurement of specific gravities. For example, using Equation 1.1, if G_{mm} is held constant, when G_{mb} changes by +0.01, V_a changes by -0.4%. From Equation 1.2, if G_{sb} and Ps are held constant, when G_{mb} changes by +0.01, VMA changes by -0.4%. Therefore, G_{mb} is a significant component in determining asphalt mixture volumetric properties, a measurement that directly affects asphalt mixture design, field compaction, and construction acceptance (Yan, 2012). Volumetric properties, such as V_a, VMA, VFA, and percent of maximum theoretical specific gravity (% G_{mm}), are calculated during the mixture design procedure (Cooley et al., 2002). Additionally, the quality control (QC) and quality assurance (QA) of compacted asphalt pavements are typically based on the contractor achieving a minimum percent compaction in the mixture during construction (Cooley et al., 2002). To properly measure this, a G_{mb} measurement must be obtained for a mixture by taking cores from the compacted lift and using them to calibrate density gauges (Cooley et al., 2002). Therefore, the accurate assessment of G_{mb} is crucial for quality asphalt pavement production and acceptance.

The conventional methods for determining the G_{mb} of asphalt specimens—saturated-surface dry (SSD) and vacuum sealing method (VSM) are limited to average values, providing average air voids percentage and density. Also, the current methods are subject to some restrictions such as aggregate maximum size and gradations. With the advancements in today's imaging technology, the decision was made to try 3D imaging techniques to measure the G_{mb} of compacted asphalt mixture specimens to determine if a more accurate measure of specimen volume could be made, in less time, than can be done with more standard methods.

1.3 Objective

Given the importance of accurately measuring asphalt mixture G_{mb} to ensure accurate measure of asphalt mixture volumetrics, this project seeks to use imaging technology to better characterize mixtures through measurement of volumetric properties with a higher degree of accuracy than can be done with current measurement techniques. Therefore, the objectives of this research are the following.

1. Develop image measurement and processing methods to identify the precise volume of both laboratory prepared gyratory specimens and field cores.
2. Use the image-determined volume to define bulk specific gravity more precisely and therefore determine the precise air void content.
3. Develop a draft standard test method for using the chosen image measuring and processing methods to accurately determine bulk specific gravity of both laboratory prepared gyratory specimens and field cores.

1.4 Organization of the Report

The report is divided into six chapters. In the first chapter, the introduction, motivation, and research objective of the study are presented. The second chapter presents a literature review of current and old methods. Chapter three provides a description of the materials and experimental plan for evaluating the candidate method. In the fourth chapter, the findings of this study are presented and discussed. The fifth chapter presents the conclusions derived from this study.

2. ASPHALT MIXTURE BULK SPECIFIC GRAVITY MEASUREMENT METHODS

The G_{mb} of an asphalt mixture is described as the ratio of the mass of a given volume of asphalt mixture to the mass of an equal volume of water at room temperature. The use of specific gravity allows conversion between volume and mass, which is important since mass is what is measured during asphalt mixture production. Several test methods have been developed to measure the G_{mb} of compacted asphalt mixtures.

2.1 Dimensional Analysis Method

The dimensional analysis method (DAM) is a simplistic volumetric method for determining the G_{mb} of compacted asphalt mixture specimens. The average height and diameter of the specimen are determined and used to calculate the specimen volume, given the specimen is a right circular cylinder. This method assumes the specimen surface is smooth, typically a poor assumption (Williams et al., 2005). The G_{mb} cannot be calculated accurately if surface irregularities are ignored. Therefore, DAM is recommended for use with cut-specimen surfaces, when the specimen surface tends to be more uniform, to minimize erroneous results.

To obtain the G_{mb} of a compacted asphalt mixture specimens with DAM, the mass and dimensions of the sample are first accurately measured (Williams et al., 2005). Equation 2.1 is used to calculate the G_{mb}.

$$G_{mb} = \frac{m_{dry}}{\left(\frac{\pi \cdot d^2}{4}\right) \cdot h \cdot \rho_w} \qquad \text{(Eq. 2.1)}$$

where:

G_{mb} = the bulk specific gravity of the sample,

M_{dry} = mass of dry sample (g),
d = average sample diameter (cm),
h = average sample height (cm), and
ρ_w = density of water at 25°C (77°F).

In this method, the height and diameter measurements are often the source of errors (Buchanan, 2000). Due to the presence of surface irregularities, this method tends to overestimate the specimen volume, and thereby the G_{mb} measurement is underestimated, as compared to its true value.

2.2 Saturated Surface Dry

Based on Archimedes concept of water displacement, the saturated-surface dry (SSD) method for determining the G_{mb} of compacted asphalt specimens has been widely used for many years (Dukatz et al., 2009). AASHTO T166 and ASTM D2726 are the standard test methods. The SSD test can only be performed on compacted asphalt specimens with water absorptions of less than 2%, so it is not recommended for specimens containing open or interconnected air voids (Williams et al., 2005). According to the standard test methods, to determine the G_{mb} of a compacted asphalt mixture specimen, the following steps are completed.

- Obtain the specimen dry mass.
- Submerge the specimen in a 25°C-water bath for 4 ± 1 minutes, then determine the specimen mass while it is still in the water.
- Remove the specimen from the water, gently pat the surface dry with a damp towel and measure the specimen mass. This mass is denoted as the SSD mass.

Once the three masses are determined, Equation 2.2 is used to calculate the compacted asphalt mixture G_{mb}.

$$G_{mb} = \frac{M_{dry}}{M_{SSD} - M_{sub}} \qquad \text{(Eq. 2.2)}$$

where:
G_{mb} = specimen bulk specific gravity,
M_{dry} = specimen dry mass(g),
M_{SSD} = specimen mass in SSD condition (g), and
M_{sub} = submerged specimen mass (g).

The proper SSD condition of a compacted asphalt mixture specimen can be difficult to determine and is therefore subject to individual interpretation, which can introduce variability and error into the results. Mixture types can also increase errors when measuring SSD condition. For example, when compared to conventional dense-graded asphalt mixtures, coarsely graded Superpave-designed and stone matrix asphalt (SMA) mixtures tend to contain larger air voids that can be more interconnected, despite being designed at 4% air voids content. Several issues have arisen when determining the G_{mb} of these "coarser" mixtures via the SSD method. Due to the internal air void structure within coarse-graded Superpave and SMA mixtures, the SSD method can produce erroneous G_{mb} measurements (Cooley et al., 2002).

Cooley et al. (2002) visualized this point as shown in Figure 2.1. Due to the larger, interconnected air voids in the coarser specimen, water can rapidly infiltrate into the specimen when it is submerged in water. However, when it is removed from the water bath, water can quickly drain from the sample, causing error in the SSD mass.

Understanding the principles of water displacement is imperative to grasping the potential error in G_{mb} determination using the SSD method. According to Archimedes' Principle, an object submerged in water has a buoyant force that corresponds to the volume of water displaced by the object. Therefore, the G_{mb} of a compacted asphalt specimen can be calculated by dividing the specimen dry mass by the specimen volume. Figure 2.2 shows the volumes of both coarse- and fine-graded compacted asphalt specimens. In Figure 2.2(a), the volume is determined based on specimen dimensions. In this case, G_{mb} measurement would be low because any surface irregularities are included as part of the volume, which leads to an overestimation of the specimen volume.

The apparent volumes of the compacted asphalt mixture specimens are shown in Figure 2.2(b). This illustration shows the specimen volumes are underestimated, because the interconnected air voids into which water can easily infiltrated are not considered as part of the specimen volume. This scenario is mostly associated with coarsely graded asphalt

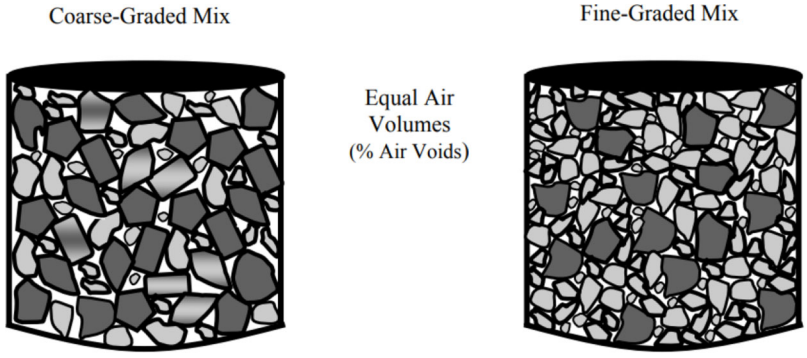

Figure 2.1 Internal void structure for coarse- and fine-graded compacted asphalt mixtures (Cooley et al., 2002).

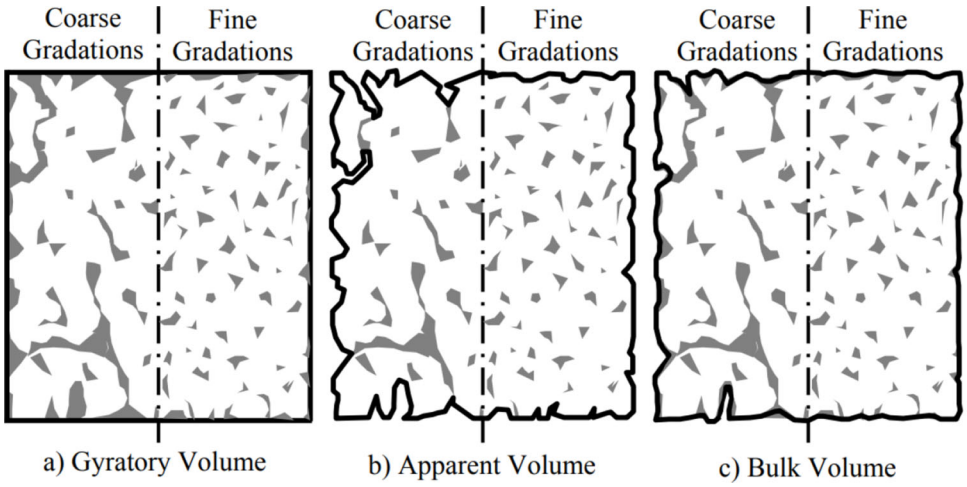

Figure 2.2 Illustration of different volumes of the internal structure of coarse- and fine-graded mixtures (Cooley et al., 2002).

mixtures. Figure 2.2(c) shows the specimen volume ideally suitable for measuring true G_{mb} as it accounts for the interconnected voids and the surface irregularities (Cooley et al., 2002). As this figure shows, the coarser mixture is more prone to water drainage from interconnected voids, resulting in inaccurate SSD mass measurement, and thereby increasing error in the volume determination of the sample by the water displacement method. As a result, a higher specific gravity value than the true value is determined (Dukatz et al., 2009). Consequently, volumetric properties such as air voids, VMA, and VFA may be overestimated due to an overestimation of G_{mb}.

2.3 Paraffin and Parafilm Methods

To overcome the problem inherent in AASHTO T166 and ASTM D2726 for compacted asphalt mixture specimens with higher absorption number (i.e., >2%), the paraffin and parafilm methods were introduced as standardized in AASTHO T275 and ASTM D1188, respectively. With these methods, the asphalt mixture specimen is either wrapped in parafilm or coated with paraffin. These methods are time-consuming, and in the case of paraffin, can be messy (Williams et al., 2005). If a specimen is to be subjected to additional testing, the parafilm method is recommended, since theoretically, the parafilm can be removed. In accordance with both AASHTO T275 and ASTM D1188, Equation 2.3 is used to calculate the G_{mb} of compacted asphalt mixture specimens.

$$G_{mb} = \frac{M_{Dry}}{\left[M_{CD} - M_{CS} - \frac{M_{CD} - M_{Dry}}{G_C}\right]} \quad \text{(Eq. 2.3)}$$

where:

G_{mb} = specimen bulk specific gravity,
M_{Dry} = uncoated specimen dry mass (g),
M_{CD} = coated sample dry mass (g),
M_{CS} = mass of coated sample submerged in water (g), and
G_C = coating material specific gravity.

2.4 Vacuum Sealing Method

The vacuum sealing method (VSM) was developed to determine the G_{mb} of compacted asphalt mixture specimens that have coarser and more open-graded aggregate gradations using a device commercially known as the "CoreLok" device. This method uses a plastic bag in which the specimen is sealed to ensure it remains dry during testing. While the method is similar to the paraffin and parafilm methods, VSM avoids the mess of paraffin and the difficulties of parafilm, plus the added advantage of more reproducible test results. Hall et al. (2001) demonstrated that VSM shows only a slight variation in multi-operator repeatability. In the VSM, compacted asphalt mixture specimen G_{mb} is calculated by a computer program based on the values determined from steps one through six. In accordance with both ASTM D6752 and AASHTO T331, Equation 2.4 is used to calculate the G_{mb} of compacted asphalt specimens.

$$G_{mb} = \frac{M_{Dry}}{\left[\left[M_{AT} + (M_{Bag} - M_{Dry})\right] - M_{SS} - \frac{M_{Bag} - M_{Dry}}{G_{Bag}}\right]} \quad \text{(Eq. 2.4)}$$

where:

G_{mb} = specimen bulk specific gravity,
M_{Dry} = unsealed specimen dry mass (g),
M_{AT} = unsealed specimen mass, after testing (g),
M_{Bag} = bag mass (g),
M_{SS} = mass of sealed specimen submerged in water (g), and
G_{Bag} = Sealing bag specific gravity.

2.5 Methods Comparison

Over the past few years, several studies have compared the SSD-based methods with alternative

standard methods for determining the G_{mb} of compacted asphalt mixture specimens. Buchanan (2000) compared the SSD method with VSM, the parafilm method, and DAM. All compacted asphalt mixture specimens were prepared by a gyratory compactor to yield specimens with a wide range of air voids contents. The experiment included fine- and coarse-graded Superpave-designed mixtures, SMA, and open-graded mixtures. Results indicate the SSD and VSM methods provide similar G_{mb} results for fine- and coarse-graded asphalt mixtures, but the data for SMA and open graded mixtures methods resulted in a higher V_a (Buchanan, 2000). It was concluded that mixtures with even low absorption (i.e., absorption $< 2\%$) are still subject to a significant error. The VSM was ultimately determined to be the most accurate method of measuring the G_{mb} of all specimens, regardless of the gradation, aggregate type, or compaction level.

A further finding of the study indicates the CoreLok-based G_{mb} measurement was somewhat variable because of the unfamiliarity of operators with the device (lack of experience) and the specimen dry mass. This latter error is introduced when the same specimen is used for CoreLok and AASHTO T166 methods (Buchanan, 2000). Several factors that contributed to the difference were CoreLok bag thickness, sample temperature, and the time sample was left sealed prior to testing (Buchanan, 2000). The authors argued that the AASHTO T166 method overestimates the G_{mb} when the water absorption of compacted asphalt mixture specimens increases. According to this study, CoreLok had a higher variability than AASHTO T166, likely due to CoreLok bags losing vacuum over time, especially when testing coarse-graded and SMA mixtures. However, Hall et al. (2001) measured the G_{mb} of various asphalt mixtures and found that VSM provides measurements with less variability than the SSD-based method.

Cooley et al., (2002) performed a comprehensive interlaboratory study to compare the G_{mb} measurement results obtained from ASSHTO T166 and VSM. Their research showed that VSM results were less precise than AASHTO T166 for most mixtures tested. The authors claimed that such enormous errors within VSM could be attributed to water leaking into the vacuum bag and the operator's lack of experience. In another study conducted by Brown et al., (2004a), it was recommended to re-weight the VSM specimen after recording the submerged specimen, since some water may leak into the vacuum bag. Also, the authors advocated a small air voids content correction factor (-0.02% V_a) when VSM is used. Williams et al. (2005) investigated the G_{mb} determination through four methods, including AASTHO T166, VSM, dimensional analysis, and gamma-ray methods. Two coarse-graded mixtures with different V_a were used and the results indicated that AASHTO T166 had the lowest variability, followed by VSM.

In the same vein, the NCHRP 9-26 project (Azari et al., 2006) was performed to estimate the precision of G_{mb} measurement by AASHTO T166 and VSM. The study concluded that mixtures with a different nominal maximum aggregate size, along with high and low absorption numbers, yielded similar precision estimates for G_{mb}. Table 2.1 from a study by Brown et al. (2004b) summarizes the recommended precision estimates for both methods.

Given the limitations of the currently available methods for determining compacted asphalt mixture specimen volumes and thereby G_{mb}, it was postulated that some form of electronic imaging might provide improved accuracy of such measurements. It has become widespread practice to use imaging technology in many fields of science in recent years. Incorporating such a technique goes beyond its initial use in biomedicine (Acharya & Ray, 2005). For instance, in 1982, digital imaging was used to quantify and analyze the stress and strain zone in the experimental study of solid mechanics (Peters & Ranson, 1982). Given this, it might be possible to use non-contact, three-dimensional (3D) scanning to accurately determine the volume of compacted asphalt mixture specimens.

2.6 3D Scanner

2.6.1 History

Three-dimensional scanning uses a digital device to collect and analyze shape and appearance data from real-world objects. The collected data is then used to construct a 3D model of the object. In an early attempt, a 3D scanner was developed to recreate the surface of an object (Abdel, 2011). The early 3D scanner models used lights, projectors, and cameras to collect data. The main problem experienced was the data processing, something that can take a great deal of time, but accuracy was thought sufficient (Stojkic et al., 2020). After 1985, an upgrade was made in which the scanner could use white light along with lasers and shadowing

TABLE 2.1
NCHRP 9-26 suggested precision estimation for the G_{mb} measurement of compacted asphalt mixture specimens (Brown et al., 2004b)

Method	Precision	Standard Deviation (1s)	Acceptable Range of Two Results (d2s)
AASHTO T166	Single operator	0.012	0.033
	Multi-laboratory	0.016	0.044
ASTM D6752	Single operator	0.013	0.036
	Multi-laboratory	0.021	0.059

Figure 2.3 Scanning a tape with the 3D scanner (Abdel, 2011).

Figure 2.4 3D scanner with contact probe (Edl et al., 2018).

to collect data on a given surface (Stojkic et al., 2020). At that time, the concern that arose was the generation of the model. Figure 2.3 shows the scanning of a tape.

Today, a variety of technologies are used for the 3D imaging acquisition. There are two main categories of scanners—contact and contactless scanner (Curless, 1999) The contactless scanner can be further divided into two major groups—active and passive scanners.

2.6.1.1 Contact scanner. Three-dimensional contact scanners commonly have a physical probe to touch the object being scanned. Generally, the object is placed on a fixed platform and the probe is attached to an arm that is manually or robotically rotated around the object. Each contact point is then measured as a cloud point in an X, Y, and Z coordinate system. The recorded points create a "cloud" of the object that can be transformed into a 3D model by using meshing techniques. Although the accuracy of contact scanning is good, the method suffers from a slow scanning rate and may not be useable with soft and delicate objects. Figure 2.4 shows one type of contact scanners. Generally, such scanners were used for quality control of products in the manufacturing process and would be very accurate. Again, the concern regarding the damage or modifying the object under scanning still exists (Abdel, 2011).

2.6.1.2 Contactless scanners. As the name implies, non-contact scanners do not need physical contact with a given object in order to complete a scan. Instead, such scanners rely on passive and active techniques to capture the object's image. The outcome of non-contact scanning appears as a cloud of captured data points that must be transformed into a 3D model via reverse engineering, virtual assembly, analysis, and other software features (Kersten et al., 2005). Non-contact active scanners radiate light or other emission, such as ultrasound or X-rays, and then detect the waves' reflections to capture points from the object surface (Amzajerdian et al., 2011). Such scanners can work in either active or passive modes.

2.6.2 Three-Dimensional Scanning for Paving Materials

To use 3D scanning for paving materials, it is first necessary to establish a set of guidelines to filter available 3D scanners, to better assess their feasibility for use in pavement material engineering. These variables include:

- accuracy,
- resolution,
- post-processing time,
- scanning time,
- ability to capture dark objects (i.e., laboratory compacted specimen),
- dimension and weight limits, and
- the capability of object auto-recognition.

For example, accuracy is important since the distance between two individual scanned points should be accurate enough to reproduce a specimen representation that can be used to measure its volume. Moreover, some specimens may have rough surfaces that may affect the final measured volume. Therefore, a high-resolution scanner will enable more precise measurements. An example of a specimen that exhibits some degree of roughness on the surface can be seen in Figure 2.5. In this figure, scans were done at two different resolutions, low and high. As indicated, the scan attributed to the high resolution resulted in a shape with more details and a more precise volume that better matches the original specimen. Such analyses highlight the importance of a scanner's resolution to capture data points.

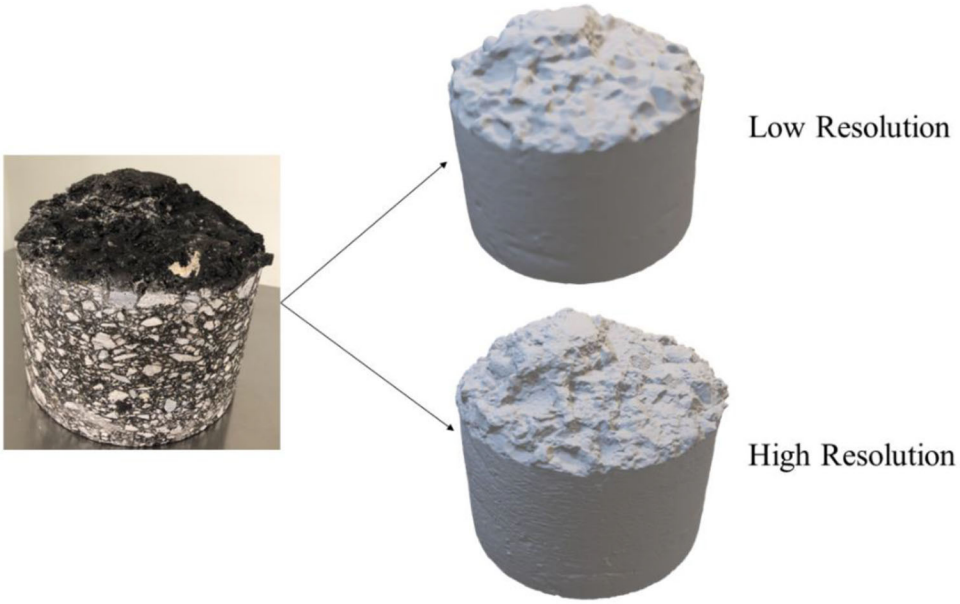

Figure 2.5 Compacted HMA specimen with a rough surface.

Another example is post-processing time, a crucial factor for use with asphalt materials. During construction, the more quickly test results can be returned, the better the decisions made. The post-processing time is highly dependent on the computer power used to mesh and render the model once scanning is complete. Since it is possible to capture tens of millions of points with one scan, the computer hardware and software must be powerful enough to process the data and construct the model in a reasonable amount of time.

Based on the literature, it is understood that improper measurement of compacted asphalt mixture G_{mb} can lead to an unfavorable mixture design resulting in premature pavement distress. The accuracy with which asphalt mixture volumetric properties are measured is critical for pavement performance. With the advancements in today's imaging technology, the decision was made to try 3D imaging techniques to measure the G_{mb} of compacted asphalt mixture specimens to determine if a more accurate measure of specimen volume could be made, in less time, than can be done with more standard methods.

3. EXPERIMENT MATERIALS, EQUIPMENT, AND TEST METHODS

3.1 Materials

In order to reasonably evaluate 3D scanner capability and accuracy for measuring the volume of compacted asphalt mixture specimens, it was necessary to test various specimen sizes and asphalt mixture types. Table 3.1 shows the experimental matrix. The factor levels for specimen sizes include specimen diameter and height, field and laboratory produced specimens, and if a specimen was cored or not (Figure 3.1). Factor levels for mixture types include standard dense-graded Superpave mixtures, along with SMA mixtures. It is important to note that laboratory-fabricated specimens are typically darker in color than cored specimens, while core specimens tend to be a lighter shade of color and have more texture. Three-dimensional scanning was used to determine the volume of test specimens, which was then used to calculate the G_{mb} of the specimens. These results were compared with those obtained using the SSD-based (AASHTO T166) and CoreLok methods.

3.2 Equipment

3.2.1 Three-Dimensional Scanner

A 3D scanner and attendant software were used to measure compacted asphalt specimen volumes. Figure 3.2 shows the scanner used. As seen in the figure, there is an automatic turntable with target markers that help the scanner better recognize the object in a shorter time period. The scanner has the following accessories:

- power adapter and cable,
- calibration board,
- calibration board bracket,
- markers,
- turntable, and
- tripod.

The scanner's technical information is summarized in Table 3.2. The minimum computer requirements suggested by the scanner manufacture are listed in Table 3.3.

TABLE 3.1
Specimen information

Mixture Type	Nominal Maximum Aggregate Size, mm (inches)	Sample Diameter (D), mm (inches)	Sample Height, (H), mm (inches)	Specimen Origination
Dense-Graded Asphalt Mixtures	9.5 (3/8)	38 (1.5)	100 (4)	LMLC, core
	9.5 (3/8)	100 (4)	150 (6)	LMLC, core
	9.5 (3/8)	150 (6)	50 (2)	FMFC, core
	9.5 (3/8)	100 (4)	150 (6)	LMLC
	12.5 (1/2)	38 (1.5)	100 (4)	LMLC, core
	12.5 (1/2)	150 (6)	50 (2)	LMLC, core
	12.5 (1/2)	150 (6)	50 (2)	LMLC
	19.0 (3/4)	38 (1.5)	100 (4)	LMLC, core
	19.0 (3/4)	150 (6)	50 (2)	FMFC, core
	19.0 (3/4)	100 (4)	150 (6)	LMLC
	19.0 (3/4)	150 (6)	50 (2)	LMLC, RS
	19.0 (3/4)	100 (4)	150 (6)	FMFC, RS
	25.0 (1)	150 (6)	50 (2)	LMLC
	25.0 (1)	38 (1.5)	100 (4)	LMLC, core
Stone Matrix Asphalt (SMA)	9.5 (3/8)	150 (6)	50 (2)	FMFC, core
	19.0 (3/4)	150 (6)	50 (2)	FMFC, core
	9.5 (3/8)	100 (4)	150 (6)	LMLC
	19.0 (3/4)	100 (4)	150 (6)	LMLC

Notes:
LMLC: The specimen was compacted in the laboratory using laboratory prepared asphalt mixture.
FMFC: The specimen was compacted in the field using asphalt-plant prepared mixture.
Core: A core was taken from the specimen.
RS: The specimen has a rough texture on the top side.

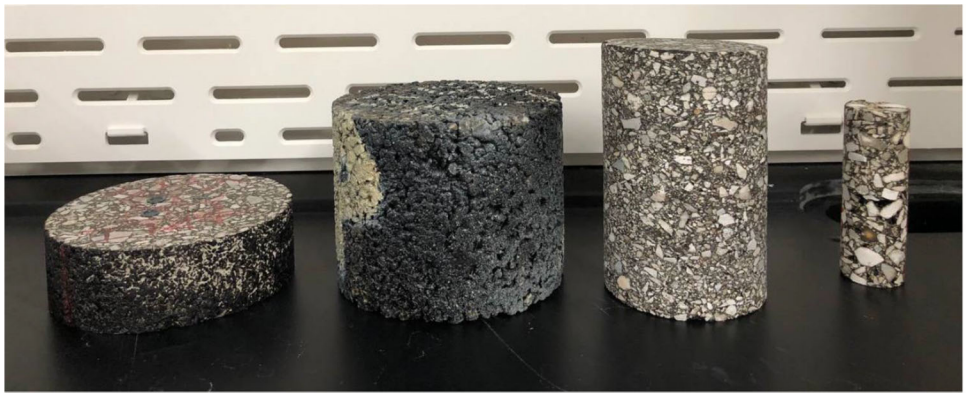

Figure 3.1 Common size of asphalt specimens used in this study.

3.3 Methodology

3.3.1 Imaging Method

The scanning system used in this experiment has three available scanning modes for measuring object volume, fixed, either with or without using a turntable to hold the object, and handheld, with either a high-density or rapid scan. Table 3.4 summarizes the advantages of each scan mode. Among these modes, the fixed scanning mode is recommended for scanning small objects with high accuracy, while the other two modes are recommended for large objects. The compacted asphalt mixture specimens were scanned in fixed mode, using a turntable. To accomplish this, the scanner was placed in a fixed position while the specimen was placed on the turntable and rotated. A software overview of the available parameters to be selected before scanning is shown in Figure 3.3. As shown, the scanning modes and features need to be selected within the scan setting. To synchronize the scanner and turntable, the "*with turntable*" should be checked. As the second input, the number of rotations to be completed by the turntable for each scanning operation is determined. Depending on the complexity of the object, the "*turntable steps*" (steps is the turntable rotations) can range from 4 to 180. Increasing the number of steps will result in a greater

Figure 3.2 3D scanner configuration.

TABLE 3.2
Technical specification of EinScan Pro HD

	Scanning Mode		
Parameters	**Handheld HD Scan**	**Rapid Scan**	**Fixed Scan**
Accuracy, mm	Up to 0.05	Up to 0.10	0.04
Scan Speed, Frames/Second	10	30	A single scan is less than 0.5 second
Degrees of Freedom, mm	100	100	100
Working Center Distance, mm	510	510	510
Light Source	LED	LED	LED
Texture Scan	Yes	Yes	Yes

TABLE 3.3
Minimum computer requirements for the 3D scanner

Item	**Minimum Requirements**
Windows	Win10 (64 bit) or higher
CPU	Intel Core i7-8700 or higher
Graphic Card	2X Series: NVIDIA GTX1060 or higher 2020 Series: NVIDIA GTX1080 or higher
Memory	8G
USB Type	USB 3.0
Resolution	1920*1080 pixels

number of measured points on the object. The higher number of scanned points, the better the measurement accuracy, but the longer the necessary post-processing time.

For each specimen, at least two scan positions are required to construct an accurate specimen model. In the fixed mode, one specimen face is never visible to the scanner. For example, the bottom surface of a cylindrical compacted asphalt mixture specimen sitting on the turntable will not be scanned. It is, therefore, necessary to scan the specimen from two distinct positions to obtain a consistent number of points across all surfaces. Doing so will generate two data sets, known as "clouds" or "clouds of points," one for each position. Figure 3.4 illustrates the scanning steps for an asphalt specimen. The software automatically aligns two clouds of points after completing the scan of two positions, and the operator is then required to specify the level of meshing, low, medium, or high. The higher the meshing level, the better the measurement accuracy. After alignment and meshing, depending on the computer's processing power, the software can take several minutes to construct the model, as shown in Figure 3.5. Once the final model has been rendered, a measurement toolbox appears in the measurement tab. Using the toolbox's measurement menu, it is possible to

TABLE 3.4
Available scan modes

Scan Mode	Technical Parameter[1]			Object Size	Weight Limits, kg
	Accuracy	Speed	Resolution		
Fixed Scan With Turntable	4	2	4	Small objects, up to 15 cm in the horizontal direction and 25 cm vertically	Up to 5
Fixed Scan Without the Turntable	4	1	4	Small objects up to 30 cm in each dimension	No limits
Handheld HD Scan	3	3	3	Large objects, up to 4 m in each dimension	No limits
Handheld Rapid Scan	4	4	2	Large objects, up to 1.5 m in each dimension	No limits

[1]Numerical scale with a range from 1 (low) to 5 (high).

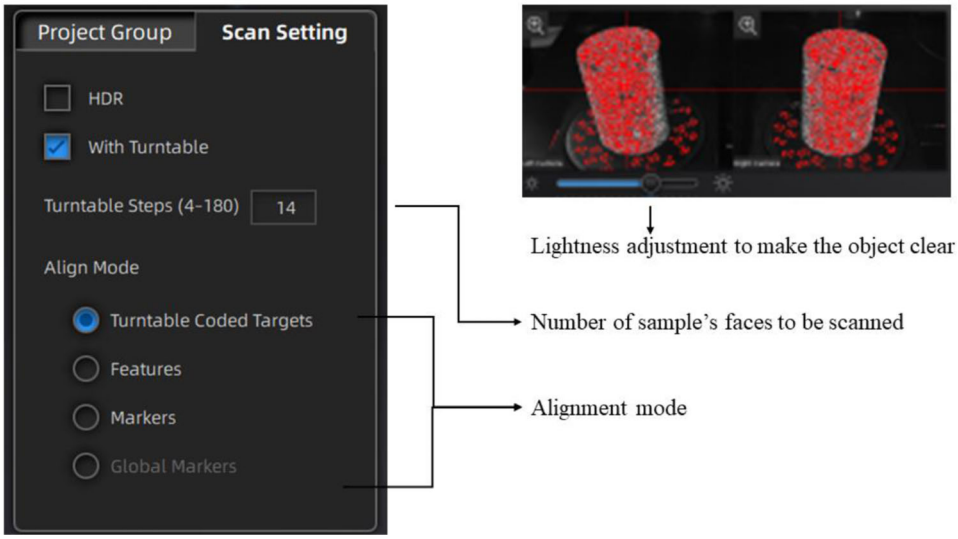

Figure 3.3 Input parameters required for fixed mode scanning.

measure the distance, surface area, and volume of the scanned specimen.

Another point of interest shown in Figure 3.4, is the time of each step. As indicated the total time required to measure the volume of a given asphalt specimen is the summation of scanning time (t_1) and post-processing time (t_2). Scanning time depends on the number of scanning positions (suggested at least two) and the number of turntable steps. After obtaining the volume, the G_{mb} can be obtained using Equation 3.1.

$$G_{mb} = \frac{M_{Dry}}{v \times \rho} \qquad \text{(Eq. 3.1)}$$

where:

G_{mb} = asphalt specimen bulk specific gravity,
M_{Dry} = asphalt specimen dry mass, (g)
v = scanner measured volume, (cm^3), and
ρ = density of water, (gr/cm^3).

Laboratory-fabricated specimens that are not cored appear totally black, due to the asphalt binder color. This can sometimes make it difficult for the scanner to recognize all specimen boundaries. If necessary, white spray paint on the specimen, creating markers on the sample, can alleviate the problem (Figure 3.6).

3.3.2 AASHTO T166 Method

The G_{mb} of the specimen was measured following AASHTO T166. To this end, the dry mass (A), SSD mass (B), and submerged mass under water (C) of the specimens were measured and used to calculate the G_{mb} (Equation 3.2).

$$G_{mb} = A/(B-C) \qquad \text{(Eq. 3.2)}$$

3.3.3 CoreLok Vacuum Sealing Method

The bulk specific gravity of asphalt specimens was measured following ASTM D6752. To do this, the appropriate bag size was selected and then weighted to the nearest 0.1 g. Then, the dry mass of the specimen was measured. After vacuuming the bag containing

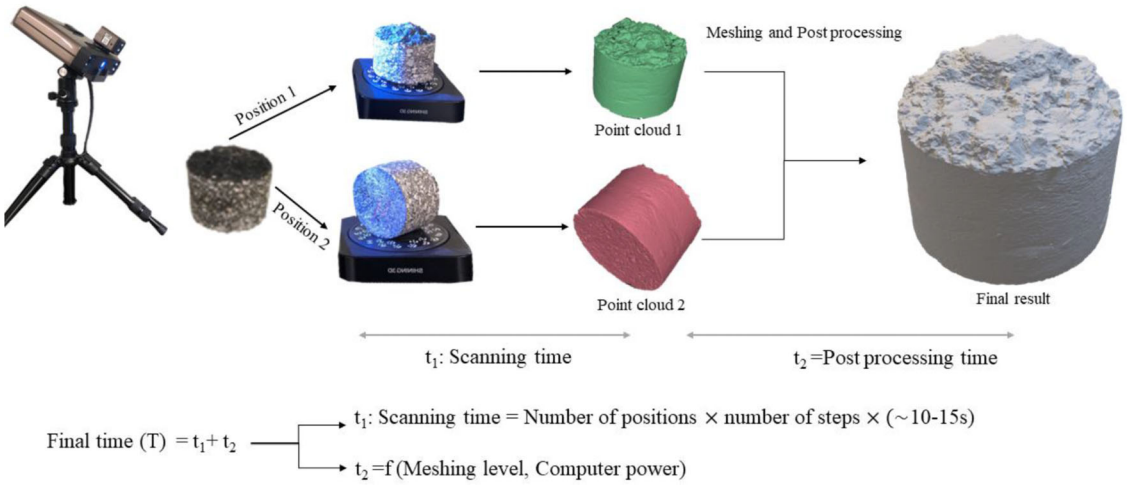

Figure 3.4 G_{mb} measurement process configuration.

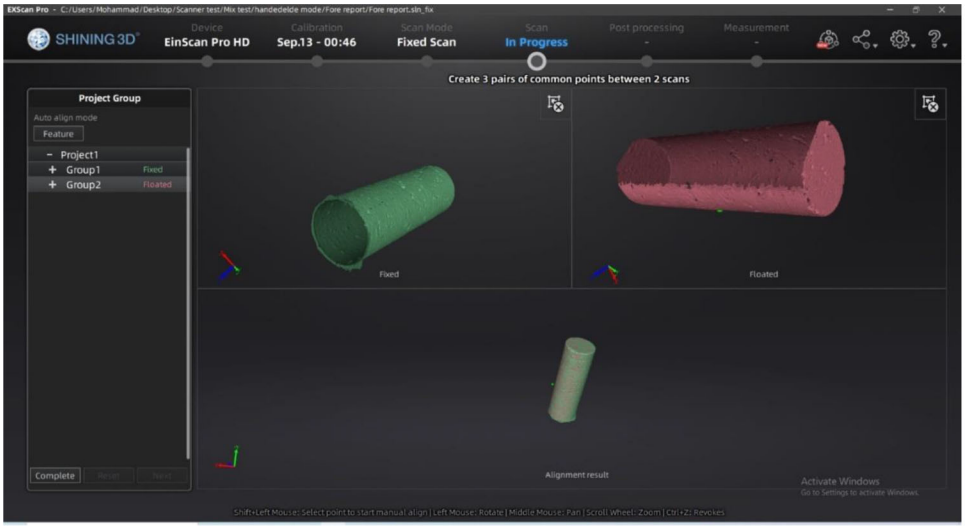

Figure 3.5 Alignment interface.

Figure 3.6 Laboratory-compacted specimen partially marked with white pen and spray.

the specimen, the sealed specimen's weight was measured to the nearest 0.1 g. Within two minutes after sealing the specimen, it was submerged into the water bath set at 25°C and maintained for 3–5 minutes, then recorded the sealed weight in water. Finally, the measured values were used as input values in an attendant software (CoreSuite) to determine the G_{mb} of the specimen.

3.4 Testing Procedures

An experimental testing design was developed to systematically evaluate the application of a 3D scanner for measuring the G_{mb} of compacted asphalt samples. To accomplish this, three phases were designed and executed, including a verification plan, a parametric study, and a comparative analysis.

3.4.1 Volume Measurement Verification Plan

In this section, two objects with pre-known volume (Figure 3.7) were tested to verify the accuracy and reproducibility of the scanner volume measurement. To this end, the volume of objects was measured in two scanning positions with 15 turntable steps per each

Figure 3.7 Two objects of pre-known volume.

position. Following this, the measured and actual volumes are compared and analyzed.

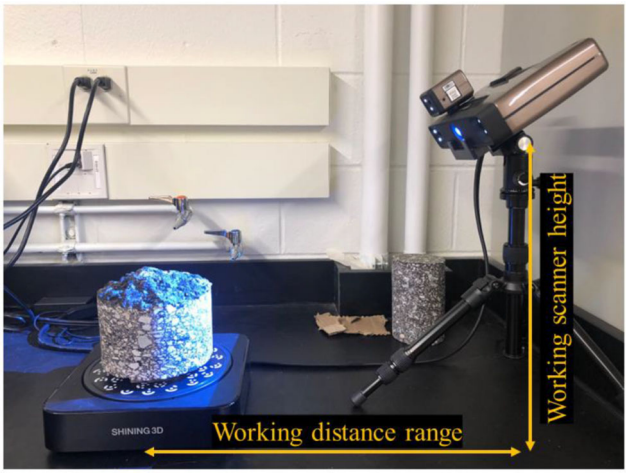

Figure 3.8 Scanner and specimens' location.

3.4.2 Parametric Study

A comprehensive testing plan was performed to determine the optimum location of scanner relative to the specimen location, the number of turntable steps, and meshing level that can be considered for an accurate measurement of an asphalt specimen's volume in a shorter amount of time.

3.4.2.1 Working distance. As part of this section, four common asphalt specimen sizes were selected to determine the working distance and elevation of the scanner relative to the specimen (see Figure 3.8). For this analysis, the number of points the scanner can measure was devised to find the optimum location of the scanner (X and Y location of the scanner from the specimen). To do so, one sample per each specimen size was scanned in a vertical range from 30 to 91 cm (12 to 36 inches) at 50 mm (2-inch) intervals. The same procedure was also done in the horizontal direction in a range from 30 to 51 cm (12 to 20 inches).

3.4.2.2 Meshing effect. The meshing process plays an essential role in engineering simulation. To obtain a more accurate volume measurement, it is crucial to generate the model with a proper meshing size. In simple words, the meshing step processes the cloud of points (i.e., at least two million points with coordination) into the final representative model. When the clouds became available, the attendant software suggests three levels of meshing: low, medium, and high detail as shown in Figure 3.9. In high detail mode, more 3D elements are used for generating the final model which is more accurate than those generated with low detail mode. Although the result will be more accurate, a substantial amount of time is typically required to generate simulated volume. Therefore, it is necessary to determine the optimum level of meshing detail for measuring the volume of asphalt samples. To this end, G_{mb} was measured by changing the meshing level at different number of turntable steps. In parallel, the processing time for each meshing detail is recorded.

3.4.2.3 Number of turntable steps. The number of steps refers to the number of stops the turntable makes during a full 360° rotation to allow the scanner to collect data. The number of steps significantly affects the scanning time since a high number of steps entails a longer scanning time. Depending on the complexity of the sample, each single step takes approximately 10–15 seconds. Additionally, longer measurement times result in a cloud with a greater number of measured points which has a significant impact on the post-processing time. Therefore, it is necessary to determine the optimum number of steps for measuring the G_{mb} of asphalt specimens in a reasonable time period. To this end, G_{mb} of asphalt specimens of different mixture types and sample sizes were measured at five turntable steps, including 10, 20, 40, 60, and 75.

3.4.2.4 Specimen size effect on required number of steps. The scanner captures points from the surface of an object. Therefore, the area of an object's surface visible to the scanner plays an important role in the number of points that can be detained at each turntable step. It is therefore necessary to determine the optimum number of turntable steps to produce a cloud containing enough points for each asphalt specimen size. To this end, three common asphalt specimen sizes were chosen, including: 38 × 100 mm (1.5 × 4 inches), 150 × 50 mm (6 × 2 inches), and 150 × 100 mm (6 × 4 inches).

3.4.3 Comparative Analysis

To evaluate the feasibility of the candidate technique for measuring G_{mb} of any asphalt specimen, a series of tests on different asphalt specimens (detailed in Table 3.1) was performed, and the measurements then compared with those obtained from AASHTO T166 and CoreLok methods. To this end, asphalt specimens

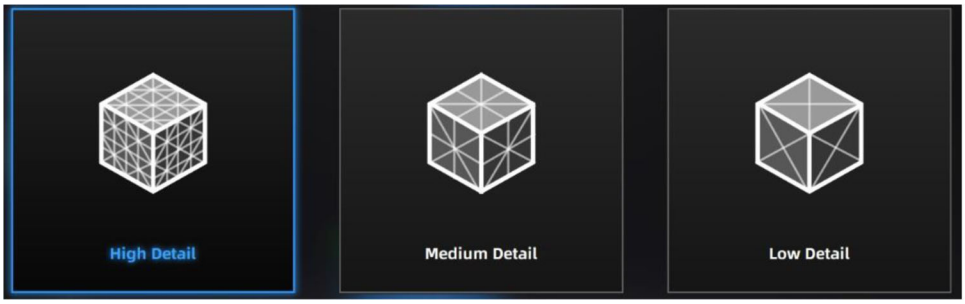

Figure 3.9 Three available meshing levels.

were first scanned, then a G_{mb} was obtained using CoreLok, and finally, specimens were subjected to AASHTO T166 testing.

3.5 Statistical Analysis

To ensure a rigorous and reliable interpretation of the study's findings, it was determined that statistical analysis using a suitable platform was necessary. In this regard, the data was analyzed using Analysis of Variance (ANOVA), which is a commonly used statistical tool that can help to identify significant differences between groups and provide a more nuanced understanding of the data.

ANOVA is a statistical technique that is widely used to compare the means of two or more groups. The output of an ANOVA test provides various measures of statistical significance, including the P- and F-values.

The P-value, also known as the probability value, is a measure of the strength of evidence against the null hypothesis. In an ANOVA test, the null hypothesis is that there is no significant difference between the means of the groups being compared. A small P-value indicates that there is strong evidence against the null hypothesis, which means that there is a significant difference between the means of the groups. Generally, a P-value of less than 0.05 is considered statistically significant.

The F-value, also known as the test statistic, is a ratio of the between-group variability to the within-group variability. In an ANOVA test, the between-group variability represents the differences in means between the groups being compared, while the within-group variability represents the differences within each group. A large F-value indicates that the between-group variability is greater than the within-group variability, which provides evidence in favor of the alternative hypothesis. If the F-value is statistically significant, it can be used to reject the null hypothesis.

4. RESULTS AND DISCUSSION

4.1 Volume Measurement Validation

The measurement results of two known-volume objects (Figure 4.1) are shown in Table 4.1. This table shows that the measured volume varies at the second digit at each replicate for the rectangular-shape plate. Considering the magnitude of the volume (~ 94 cm^3), such small deviation is negligible. The same finding also is observed for the disk-shape object. Moreover, the difference between the actual and average measured volume is less than 0.03% for both objects. This analysis appears to confirm the high accuracy of the 3D scanner in measuring the volume of an object with a high reproducibility.

An interesting aspect of the scanning ability to produce more accurate data is the 3D scanner's ability to distinguish the thickness of marked lines as shown in Figure 4.2, confirming the high accuracy of the scanning when measuring the volume of the object.

4.2 Parametric Study

4.2.1 Working Distance

Table 4.2 shows the testing condition at different vertical and horizontal working distances (defined in Figure 3.8) of the scanner from the specimen. There are five testing conditions, ranging from failed to excellent. If the scanner is placed less than 30 cm (12 inches) from the specimen, the scanner cannot recognize the specimen regardless of specimen size. Similarly, if the working distance exceeds 71 cm (28 inches), the scanner again fails to recognize the specimen. However, the

Figure 4.1 Scan results of known objects.

TABLE 4.1
Measurement result of known objects

Object		Plate	Disk
Real Volume, cm^3		94.530	168.213
Measured Volume, cm^3	Rep. 1	94.564	168.117
	Rep. 2	94.591	168.223
	Rep. 3	94.523	168.239
	Standard Deviation	0.048	0.066
	Average	94.559	168.193
Difference, cm^3		0.029	0.019
Difference, %		0.030	0.010

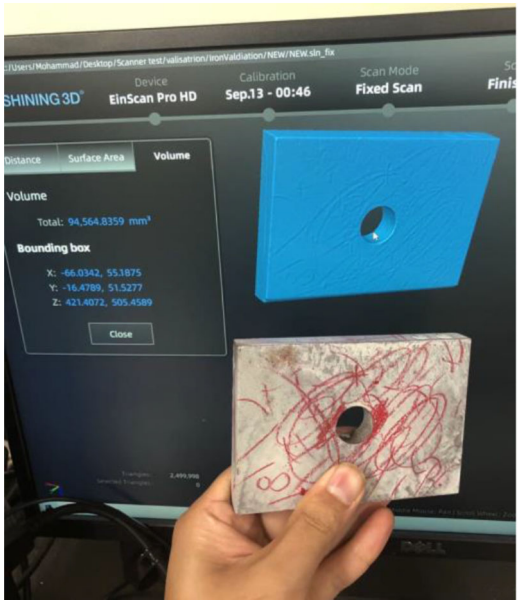

Figure 4.2 Appearance of the scanned steel plate compared to actual plate.

scanner is able to detect the specimen within a specified working distance depending on the specimen dimensions. Table 4.2 indicates that the scanner working condition depends on the specimen size; the scanner must be placed at a greater distance from the specimen as the specimen dimensions increase.

The data in Table 4.3 shows the information related to each testing condition for each specimen size. To define a criterion for evaluating the testing condition, it was decided to scan each asphalt specimen to reach a cloud containing a certain number of points, i.e., one million points for 38 × 100 mm specimen size. The data show that 57 turntable steps are required to produce two clouds, each containing one million points if the testing condition is fair. Switching the testing condition from fair to excellent reduces the number of steps to 20. A reduction of this magnitude would save 15 minutes in scanning time for 38 × 100 mm specimen size. This explanation extends to the other three specimen sizes shown in the table. Additionally, the data indicate the device is able to capture up to 400,000 points per scan step, depending on specimen size.

Finally, Table 4.4 summarizes the optimal scanner distance for each specimen size. The results suggest that if the sample is placed within the optimum range, the scanner is able to capture the highest possible points per each turntable step that results in a significant time saving. Increasing the number of points measured by a scanner reduces the number of steps required for a given object. Such a reduction can significantly reduce the necessary scan time without compromising the accuracy of volume measurement.

4.2.2 Meshing Level

To demonstrate the effect of meshing level on G_{mb} measurement, Figure 4.3 shows G_{mb} results as a function of the number of steps for three meshing levels. Comparing medium and high meshing levels visually reveals no significant differences, whereas comparing low and medium meshing levels at all steps reveals very small differences. This might be due to a simplification of texture, resulting in a slight change in the volume of the specimen. A statistical analysis on the data shown in this figure, reveals that the difference between the low and medium meshing levels is statistically significant (p-value $0.004 < 0.050$) for all turntable steps. There is no statistically significant difference between the medium and high meshing levels at any number of steps (P-value: $0.993 > 0.050$).

Obtaining the final image model requires a great deal of time, which is why the meshing step is so critical. As a result of more steps being taken, a greater number of points are produced, resulting in a longer processing time. Table 4.5 provides an indication of the post-processing time involved in meshing and constructing the model associated with the data presented in Figure 4.3. Since there is no significant G_{mb} difference between the medium and high meshing level, switching the meshing level from high to medium can significantly decrease processing time. For 20 or 40 turntable steps, this decreases the processing time from approximately 35–45 minutes down to 7–8 minutes while providing adequate information. Thus, the medium meshing level is appropriate for measuring the G_{mb} of asphalt specimens.

4.2.3 Number of Steps

Figure 4.4 displays the results of G_{mb} measurements for various dense-graded mixtures: 9.5-, 12.5-, 19.0- and 25.0-mm. The data indicate the 12.5-mm mixture has the highest standard deviation at 10 steps. Despite being high in comparison to the others, the range is extremely narrow, i.e., 0.010. However, the G_{mb} remains nearly constant after a total of 20 turntable steps per each scanning position, according to the results.

Table 4.6 shows the results of an ANOVA statistical analysis performed on this data at a 0.95

TABLE 4.2
Identified working location of scanner for four specimen sizes

Sample Size	38 × 100 mm (D × H)						
Scanner Height, cm (inches)	Scanner Horizontal Working Distance, cm (inches)						
	30 (12)	41 (16)	51 (20)	61 (24)	71 (28)	81 (32)	91 (36)
30 (12)	Failed	Fair	Excellent	Failed	Failed	Failed	Failed
36 (14)	Failed	Failed	Excellent	Fair	Failed	Failed	Failed
41 (16)	Failed	Fair	Good	Fair	Failed	Failed	Failed
46 (18)	Failed	Fair	Good	Poor	Failed	Failed	Failed
51 (20)	Failed	Poor	Fair	Failed	Failed	Failed	Failed
Sample Size	**150 × 50 mm (D × H)**						
Scanner Height, cm (inches)	Scanner Horizontal Working Distance, cm (inches)						
	30 (12)	41 (16)	51 (20)	61 (24)	71 (28)	81 (32)	91 (36)
30 (12)	Failed	Failed	Failed	Failed	Failed	Failed	Failed
36 (14)	Failed	Failed	Good	Fair	Failed	Failed	Failed
41 (16)	Failed	Failed	Excellent	Fair	Poor	Failed	Failed
46 (18)	Failed	Poor	Excellent	Fair	Failed	Failed	Failed
51 (20)	Failed	Failed	Fair	Poor	Failed	Failed	Failed
Sample Size	**150 × 100 mm (D × H)**						
Scanner Height, cm (inches)	Scanner Horizontal Working Distance, cm (inches)						
	30 (12)	41 (16)	51 (20)	61 (24)	71 (28)	81 (32)	91 (36)
30 (12)	Failed	Failed	Failed	Failed	Failed	Failed	Failed
36 (14)	Failed	Failed	Failed	Poor	Failed	Failed	Failed
41 (16)	Failed	Failed	Failed	Excellent	Failed	Failed	Failed
46 (18)	Failed	Failed	Good	Excellent	Poor	Failed	Failed
51 (20)	Failed	Failed	Excellent	Good	Failed	Failed	Failed
Sample Size	**100 × 150 mm (D × H)**						
Scanner Height, cm (inches)	Scanner Horizontal Working Distance, cm (inches)						
	30 (12)	41 (16)	51 (20)	61 (24)	71 (28)	81 (32)	91 (36)
30 (12)	Failed	Failed	Failed	Failed	Failed	Failed	Failed
36 (14)	Failed	Failed	Failed	Failed	Failed	Failed	Failed
41 (16)	Failed	Failed	Fair	Fair	Failed	Failed	Failed
46 (18)	Failed	Poor	Good	Excellent	Failed	Failed	Failed
51 (20)	Failed	Failed	Good	Excellent	Failed	Failed	Failed

confidence level. As can be seen, the P-value for all mixtures is higher than 0.050, implying there is no statistically significant difference between G_{mb} measurements at any of the number of steps. Moreover, it can be concluded that the mixture type has no effect on the variability of measured G_{mb}, since all P-values are higher than 5%. On the other hand, the F-value shows the mean G_{mb} variation between the number of steps. Higher F-values suggest higher mean variation. The F-value of the 9.5-mm mixture is the highest, implying that there is some slight G_{mb} variation within the number of steps for this particular mixture.

Since the number of steps used does not significantly affect the G_{mb} measurement, it will make sense to keep the number of steps as low as possible, to reduce scanning and post-processing time. Given the higher standard deviation of measurement at 10 steps, it seems reasonable to select 20 turntable steps as adequate to measure accurate volumes, and therefore accurate G_{mb} values for all mixtures.

4.2.4 Specimen Size

Figure 4.5 shows the G_{mb} measurements of three sample sizes at different numbers of turntable steps. Comparing Figures 4.5(a) and (b), it is evident there is negligible standard deviation after 20 steps, suggesting that the process is highly reproducible. The ANOVA results of this data are presented in Table 4.7. There is statistically significant difference of G_{mb} measurement for the 150 × 50 mm (diameter × height) specimen at different number of steps ($0.010 < 0.050$), while no significant differences are noticed for the other specimen dimensions. Figure 4.5(b) suggests this significant difference in test results is largely due to the G_{mb} measurement at 10 steps. This explanation is supported

TABLE 4.3
Scanning time associated with each testing condition and specimen size combination

Sample Size				
38 × 100 mm (D × H)				
Test Condition	**Testing Description**	**Number of Recorded Points Per Step**	**Number of Steps**	**Time (min)**
Failed	Not recognized	N/A	–	–
Poor	Missing some parts of the specimen	N/A	–	–
Fair	Feasible	35,000	57	23
Good	Feasible	60,000	34	14
Excellent	Feasible	100,000	20	8
150 × 50 mm (D × H)				
Test Condition	**Testing Description**	**Number of Recorded Points Per Step**	**Number of Steps**	**Time (min)**
Failed	Not recognized	N/A	–	–
Poor	Missing some parts of the specimen	N/A	–	–
Fair	Feasible	180,000	46	20
Good	Feasible	300,000	27	11
Excellent	Feasible	400,000	20	8
150 × 100 mm (D × H)				
Test Condition	**Testing Description**	**Number of Recorded Points Per Step**	**Number of Steps**	**Time (min)**
Failed	Not recognized	N/A	–	–
Poor	Missing some parts of the specimen	N/A	–	–
Fair	Not recognized	N/A	–	–
Good	Feasible	180,000	39	16
Excellent	Feasible	350,000	20	8
100 × 150 mm (D × H)				
Test Condition	**Testing Description**	**Number of Recorded Points Per Step**	**Number of Steps**	**Time (min)**
Failed	Not recognized	N/A	–	–
Poor	Missing some parts of the specimen	N/A	–	–
Fair	Feasible	70,000	71	29
Good	Feasible	100,000	50	20
Excellent	Feasible	250,000	20	8

TABLE 4.4
Optimal specimen distance from the scanner

Sample Size, Diameter × Height, mm (inches)	Working Distance Range, cm (inches)	Optimum Distance from Scanner, cm (inches)	Working Scanner Height, cm (inches)	Optimum Scanner Height, cm (inches)
38 × 100 (1.5 × 4)	30–61 (12–24)	51 (20)	30–51 (12–20)	30–36 (12–14)
150 × 50 (6 × 2)	41–61 (16–24)	51 (20)	36–51 (14–20)	41–46 (16–18)
150 × 100 (6 × 4)	41–71 (16–28)	51–61 (20–24)	36–51 (14–20)	41–46 (16–18)
100 × 150 (4 × 6)	41–61 (16–24)	61 (24)	41–51 (16–20)	46–51 (18–20)

by the F-value of the 150 × 50 mm specimen. Its value is higher than the other two, meaning there is significant variation among the average G_{mb}. Therefore, the use at least 20 turntable steps for scanning and determining the G_{mb} of 150 × 50 mm specimens is recommended. Moreover, Figure 4.5(c) shows little deviation at all number of turntable steps, which is likely because the sample dimension is the smallest. The G_{mb} deviation is around 0.001 for the 150 × 50 mm and 150 × 100 mm specimen sizes and increases to 0.005 for the 38 × 100 mm specimens, at 20 turntable steps.

Given the parametric study results, take all the result and discussion into account to end up the parametric investigation section, it is, therefore, suggested that 20–40 turntable steps are an adequate range for

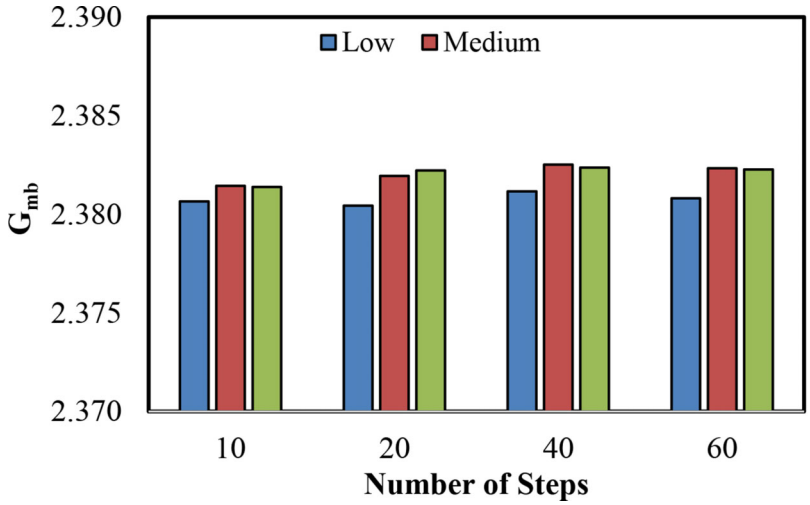

Figure 4.3 The effect of meshing level on G_{mb} at different number of steps.

TABLE 4.5
Post-processing time at different meshing and number of steps

Number of Steps	Post-Processing Time (minutes) at Three Meshing Levels		
	Low	Medium	High
10	4	6	21
20	6	7	33
40	6	8	46
60	9	22	60

measuring G_{mb} of asphalt specimen in an excellent testing condition at medium meshing level. Considering the scanning and post-processing times, it commonly takes about 10–15 minutes to get the final G_{mb} based on the suggested test inputs. Again, an amount of this magnitude is highly dependent on the computing power.

4.3 Comparative Analysis

To evaluate the feasibility of the candidate scanning method, a comparative study that compares the G_{mb} measurement obtained from the candidate scanning technique with those obtained from the AASHTO T166 and CoreLock VSM methods was completed using asphalt specimens of various mixture and specimen types.

4.3.1 Dense-Graded Mixtures

Figure 4.6 shows G_{mb} measurement for asphalt specimens fabricated from various types of dense-graded asphalt mixtures. The results indicate the scanner-measured G_{mb} has the least variation among the three measurement methods, regardless of the mixture type. The AASHTO T166 method has the widest standard error range, while the CoreLok method error falls between the scanner and AASHTO T166. The wider variation in the AASHTO T166 method may be due to measurement of specimen mass in the SSD condition, which can greatly vary for each replicate. The scanner-measured G_{mb} appears approximately equal to the CoreLok-measured G_{mb}.

Table 4.8 presents the ANOVA test results to statistically analyze differences between the scanner measurement and traditional methods. The results indicate no significant difference (P-value $>$ 0.05) between the scanner and CoreLok results for all four mixture types. Furthermore, the low F-values resulting when the scanner and CoreLok methods are compared suggests there is statistically no significant difference between the mean G_{mb} measured by the two methods.

When comparing the scanner and T166 methods, Table 4.8 shows a significant difference (P-value $<$ 0.05) between the G_{mb} measurements for the specimens containing the larger aggregate sizes, 19.0- and 25.0-mm. The higher F-values for these mixtures also indicates a significant mean variation between G_{mb} measured by the methods. However, for the smaller aggregate size mixtures (9.5- and 12.5-mm), the data show the scanner and T166 methods do not statistically differ.

Lastly, Figure 4.6(d) shows a large difference between G_{mb} measured by T166 and the other two methods. It was determined that this is a result of high absorption for the 25.0-mm mixture specimens. This particular mixture had water absorption values of more than 4%, exceeding the maximum recommended limit for the test.

4.3.2 Stone Mastic Asphalt

The surface of SMA mixtures tend to be fairly "open-graded," which can result in erroneous results when T166 is used to determine G_{mb}. Thus, only the scanner and CoreLok methods were used obtain G_{mb} values for the SMA mixtures. The results for two SMA mixtures, SMA 9.5- and 19.0-mm, are shown in Figure 4.7. The figure shows the scanner-measured G_{mb} falls within the

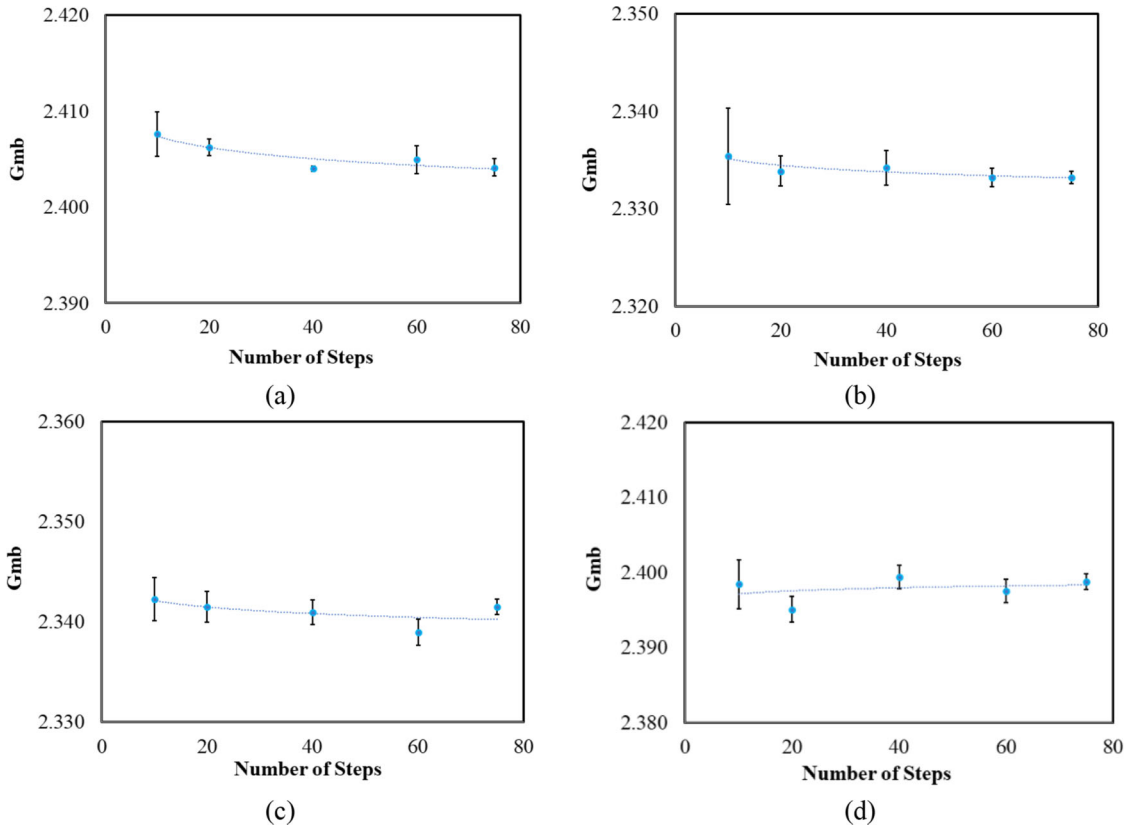

Figure 4.4 Effect of turntable steps on G_{mb} for various dense-graded mixtures: (a) 9.5-mm, (b) 12.5-mm, (c) 19.0-mm, and (d) 25.0-mm.

TABLE 4.6
ANOVA test result at all number of turntable steps

Mixture	F-value	P-value
9.5-mm	1.294	0.336
12.5-mm	0.131	0.968
19.0-mm	0.727	0.593
25.0-mm	0.746	0.583

CoreLok measurement range and has less variability, especially for the SMA 9.5-mm. Moreover, the SMA 19.0-mm results display a wider variation in CoreLok data than does the SMA 9.5-mm mixture, which may reflect the larger aggregate size.

Table 4.9 presents the ANOVA results for the SMA data, which indicates no statistically significant difference between the scanner and CoreLok methods for either mixture size (P-value $>$ 0.05). When comparing F-values, there is a small variation in mean G_{mb} for the SMA 19.0-mm specimens. In spite of this, neither the scanner nor CoreLok measurement variation exceeds 0.010.

Since all the results discussed so far have been obtained for laboratory-fabricated specimens, it is expected that the candidate method could also be used for field-cored samples. This brings us to the next topic of discussion, measuring the G_{mb} of collected field-cored specimens.

4.3.3 Field-Cored Specimens

Figure 4.8 illustrates the results of G_{mb} measurements on field-cored specimens. According to Figure 4.8(a, b), the scanner measurements appear to show the least variation of the three methods and are within the range of the other two methods. The ANOVA results indicate there is no statistically significant difference between the three methods. In terms of variability, the scanner measured G_{mb} F-value as compared to the T166 data is relatively high (5.879), indicating there is a significant difference between the mean scanner-measured and T166-measured G_{mb} values for the dense-graded 9.5-mm specimens (Figure 4.8(a)). Moreover, the AASHTO T166 method exhibits the greatest variability of the three methods, possibly due to testing operations and the method's reliance on SSD condition.

As shown in Figure 4.8(c) and (d), the scanner measurements are nearly identical to the CoreLok measurements for both SMA mixtures. The ANOVA results (Table 4.10) indicate there is no statistically significant difference between scanner and CoreLok G_{mb} measurements for the two SMA mixtures. Further examination of P-value shows that the P-value of SMA 19.0-mm is smaller than that of SMA 9.5-mm (0.080 $<$ 0.095), indicating the scanner has a relatively greater difference in G_{mb} measurement with CoreLok for larger aggre-

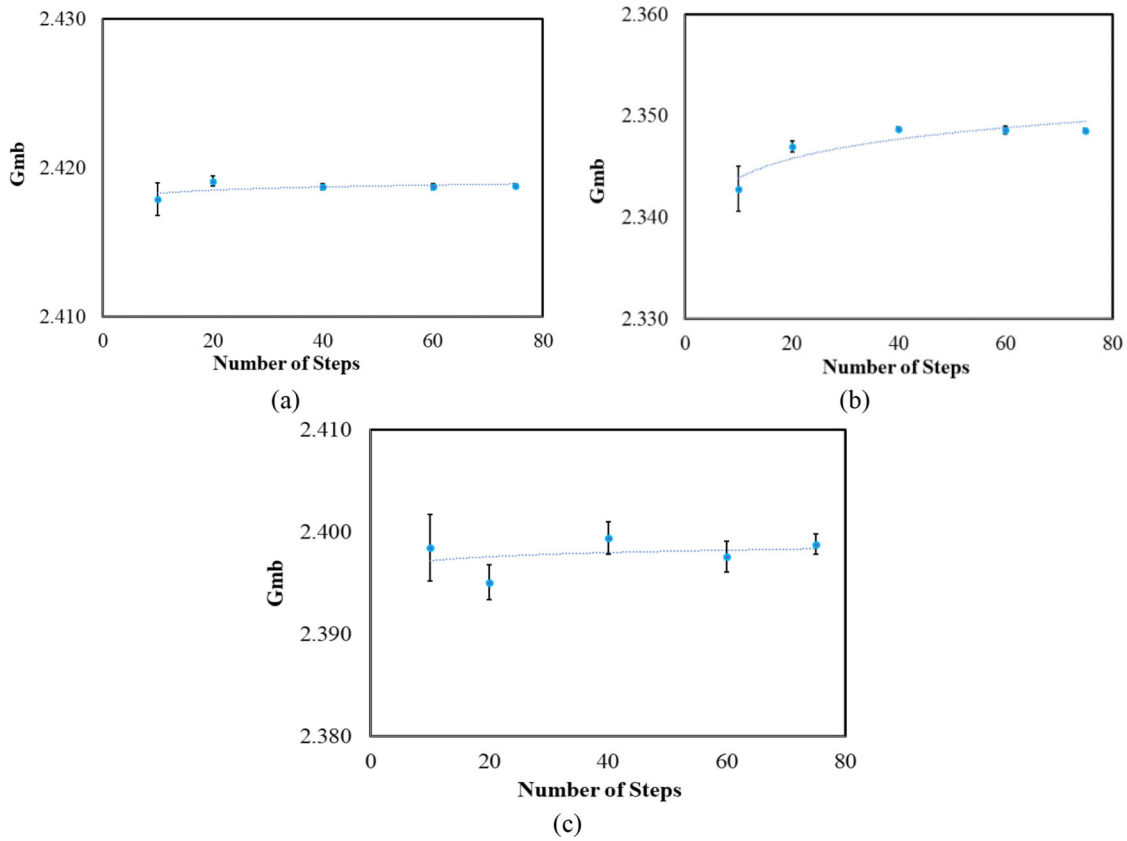

Figure 4.5 Measured G_{mb} as a function of turntable steps for various specimens' sizes: (a) 150 × 100 mm, (b) 150 × 50 mm, and (c) 38 × 100 mm.

TABLE 4.7
ANOVA test result of sample size effect on G_{mb} measurement

Sample Size, mm	F-value	P-value
150 × 100	0.729	0.583
150 × 50	5.922	0.010
38 × 100	0.746	0.592

gate size mixtures. Perhaps this is because field-cored specimens, especially those with larger aggregate particles, have a rougher surface than specimens containing smaller aggregate sizes. These larger aggregate particles and resultant rougher surfaces can make the CoreLok vacuum process less efficient, due to some air voids remaining inside the plastic bag once the vacuum has been applied. This will affect the mass of the specimen in water.

4.3.4 Water Absorption

The G_{mb} values were measured for a set of asphalt mixture specimens having varying water absorption values. The results are shown in Figure 4.9. The AASHTO T166 method was only used for specimens having less than 2% water absorption. As shown in the figure, the scanner measurement appears unaffected by absorption characteristics. The ANOVA results in Table 4.11 show no statistically significant differences between the three methods. Further assessment shows the F-value of specimens with 0.98 absorption percentage is relatively high (7.498) when comparing the scanner and CoreLok measurements, implying there is a small difference in G_{mb} variation range measured by CoreLok versus those obtained via scanner.

4.3.5 Rough Texture

Figure 4.10 illustrates the G_{mb} measurement of a specimen having a rough surface. The results show a significant difference between the CoreLok and the other two methods. To statistically test this difference, an ANOVA test was completed, the results of which are shown in Table 4.12. These results indicate that both the mean CoreLok-measured G_{mb} and the range variation are statistically different from the scanner-measured results (P-value < 0.05). The G_{mb} measure-

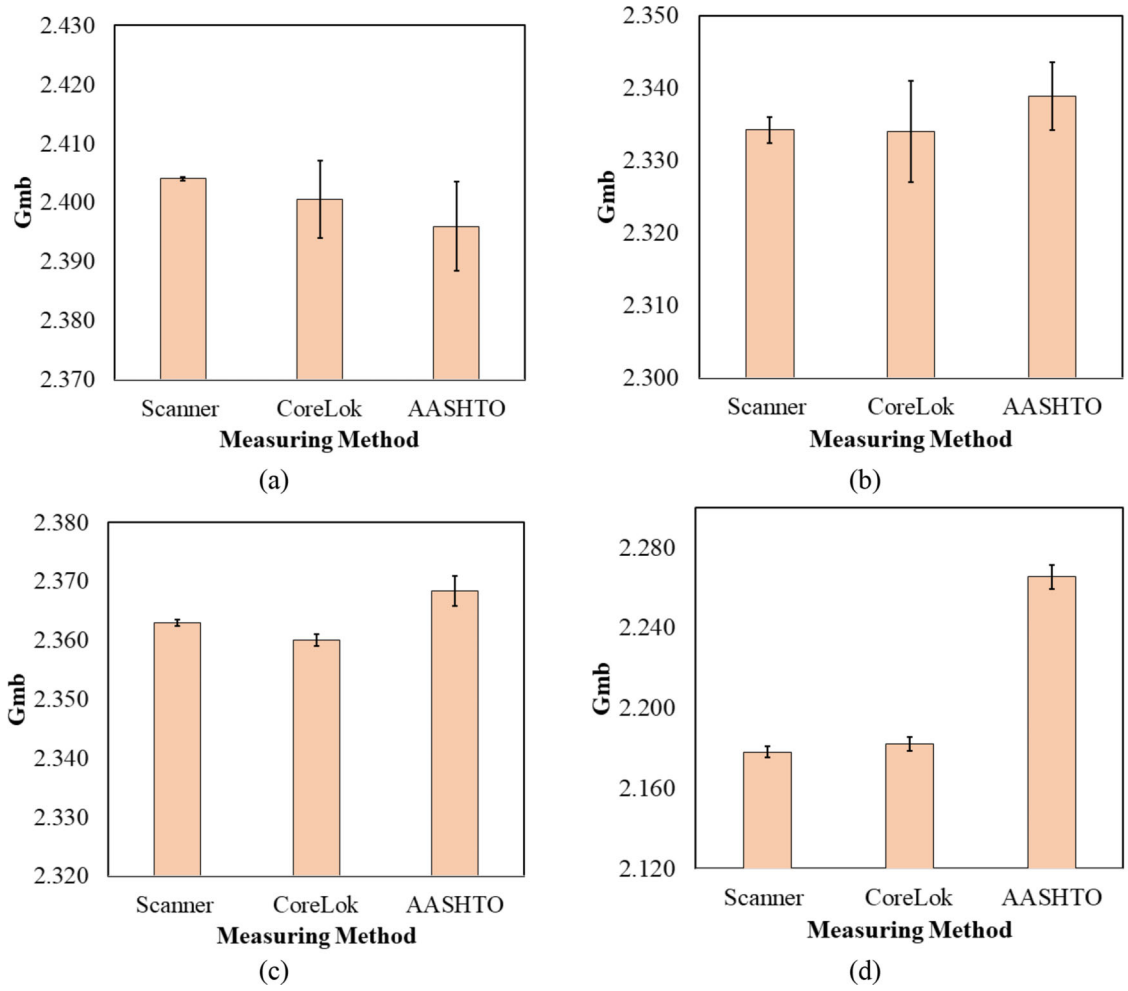

Figure 4.6 G_{mb} results obtained from variou methods for different dense-graded mixture types: (a) 9.5-mm, (b) 12.5-mm, (c) 19.0-mm, and (d) 25.0-mm.

TABLE 4.8
ANOVA test results for different dense-graded mixtures

		Secondary Method			
		CoreLok		AASHTO T166	
Primary Method	Mixture Type	F-value	P-value	F-value	P-value
Scanner	9.5-mm	0.529	0.520	2.073	0.245
	12.5-mm	0.002	0.970	1.208	0.352
	19.0-mm	0.300	0.622	68.420	0.004
	25.0-mm	0.007	0.939	158.059	0.001

ments determined by the scanner and T166 are not statistically different.

Further assessment of G_{mb} tests explain possible sources of errors in the CoreLok method. First, as seen in Figure 4.11(a), after vacuuming to remove air from the plastic bag, air voids can remain in the sealed bag. This will affect the measurement of specimen mass in water. The second cause of the error can be a water leak into the bag after the vacuum has been applied (Figure 4.11(b)). Again, this will result in a measurement error in the specimen mass in water. The scanner method is a good alternative for field specimens with rough textures. Figure 4.12 shows the measured volume of a rough-surface specimen.

4.3.6 General Analysis

Lastly, Figure 4.13 shows the G_{mb} measurement from the scanner compared to both the CoreLok and T166 methods. These plots contain all the data, regardless of mixture type and aggregate sizes. Both plots show scanner measurements within a ± 0.01 range

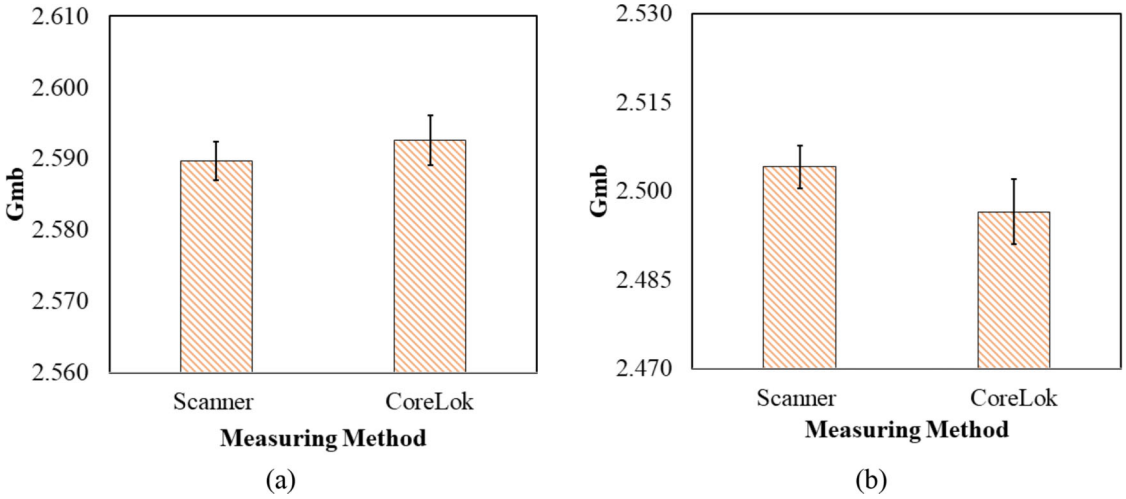

Figure 4.7 Scanner and CoreLok G_{mb} measurement results for (a) SMA 9.5-mm and (b) SMA 19.0-mm.

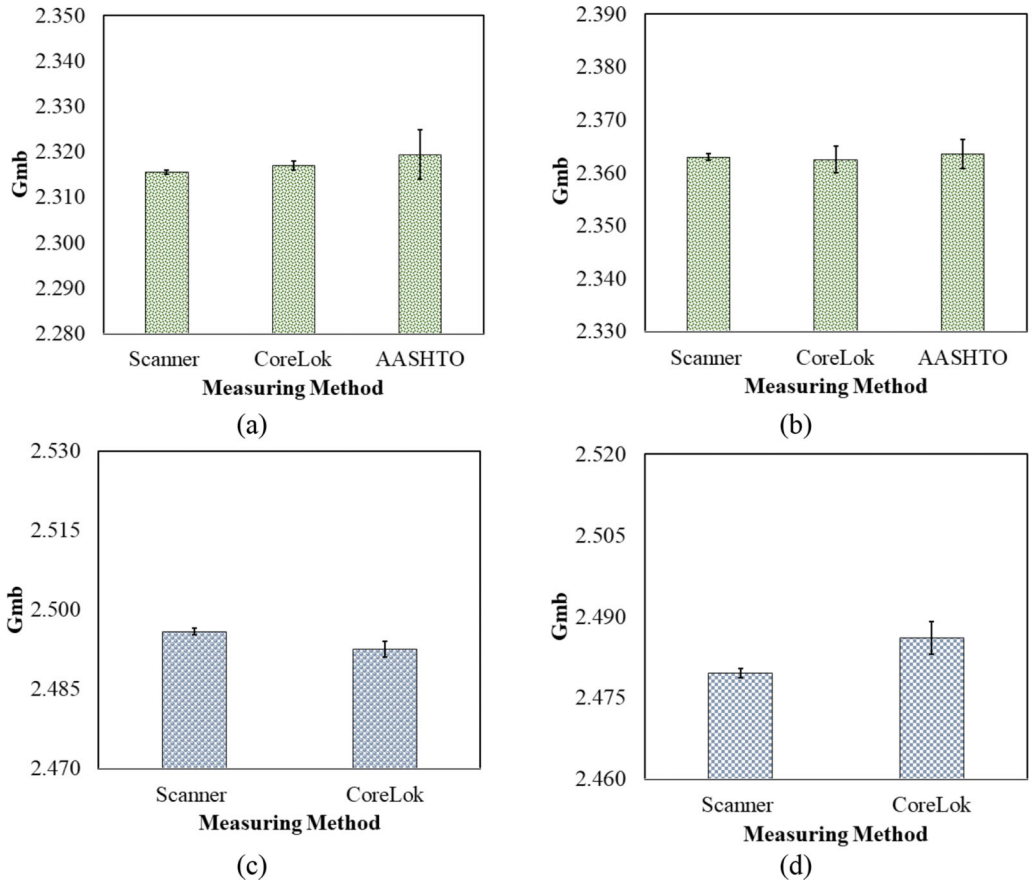

Figure 4.8 G_{mb} results for field cores specimens: (a) 9.5-mm dense graded, (b) 19.0-mm dense graded, (c) SMA 9.5-mm, and (d) SMA 19.0-mm.

TABLE 4.9
ANOVA test result of SMA mixtures

		CoreLok Method	
Primary Method	**Mixture's NMAS**	**F-value**	**P-value**
Scanner	9.5	0.416	0.565
	19.0	1.503	0.308

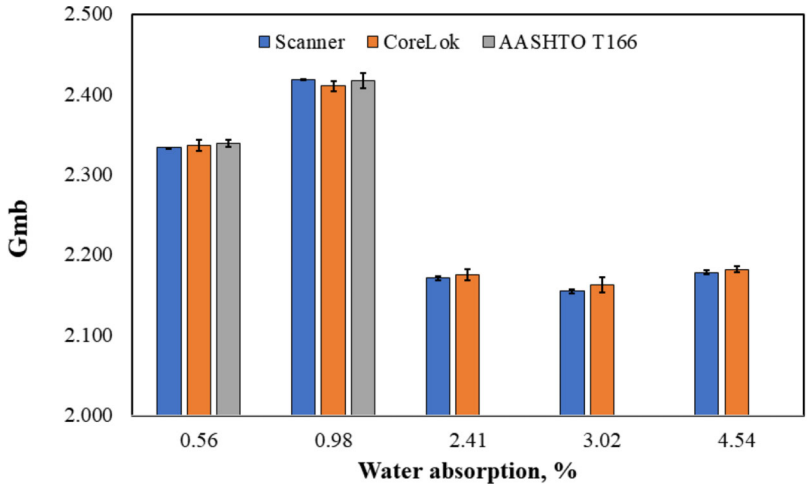

Figure 4.9 G_{mb} measurements for mixture specimens with different water absorption percentages.

TABLE 4.10
ANOVA test result for G_{mb} measured from field cored specimens

			Secondary Method			
			CoreLok		AASHTO T166	
Primary Method	Mixture Type	Mixture Size, mm	F-value	P-value	F-value	P-value
Scanner	Dense-graded	9.5	1.328	0.333	5.879	0.094
		19.0	0.058	0.826	0.798	0.438
	SMA	9.5	5.833	0.095	N/A	N/A
		19.0	6.805	0.080	N/A	N/A

TABLE 4.11
ANOVA results for G_{mb} values of asphalt mixture specimens having various water absorption percentages

		Secondary Method			
		CoreLok		AASHTO T166	
Primary Method	Absorption, %	F-value	P-value	F-value	P-value
Scanner	0.56	0.007	0.938	2.236	0.232
	0.98	7.498	0.071	0.892	0.415
	2.41	0.140	0.733	N/A	N/A
	3.02	2.010	0.251	N/A	N/A
	4.54	1.640	0.290	N/A	N/A

of both other methods' results. Again, the higher variability of T166 can be seen in the distribution of points close to range boundaries in Figure 4.13(b).

The precision estimates for all measurement methods used in the research study are summarized in Table 4.13. The results show the Scanner method had the best precision during replication, in comparison to the other two methods, AASHTO T166 and CoreLok. One possible explanation for this finding is that the Scanner method is less operator-dependent than the other two methods. This may have resulted in lower variation between the replicates, contributing to the lower precision estimate.

4.4 Cost Analysis

The research team was tasked with assessing the costs associated with using a scanner versus a CoreLok device. To do so, a quote was obtained for the same model scanner used in this study along with its necessary accessories and compared the cost with the cost of using a CoreLok device. This comparison was then summarized in Table 4.13, which provides a breakdown of the costs associated with each option.

As seen in Table 4.14, the equipment cost of the proposed method (using the scanner) is approximately similar to the cost of using a CoreLok device. However, it's important to note that over the life of the

TABLE 4.12
ANOVA test results for rough surface specimen

Primary Method	ANOVA Parameters	Secondary Method	
		CoreLok	AASHTO T166
Scanner	P-value	0.002	0.845
	F-value	56.195	0.043

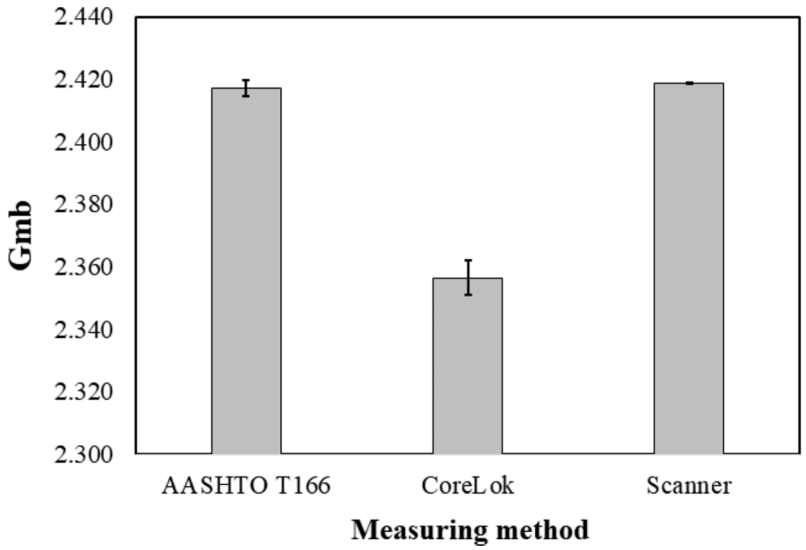

Figure 4.10 G_{mb} measurement of rough surface specimen.

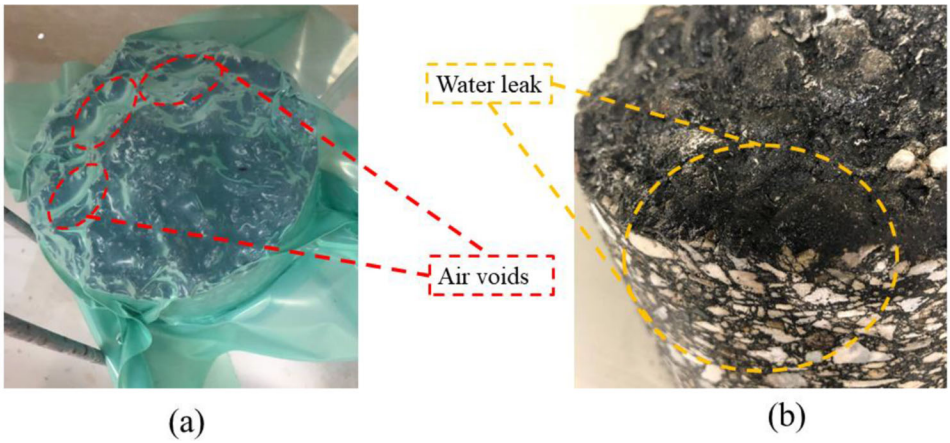

Figure 4.11 CoreLok error sources: (a) air voids present, and (b) water leak into the sealed bag.

equipment, the scanner may actually save money. This is due to the continued cost of bags for the CoreLok, which can add significant costs over time. By contrast, the scanner does not require such ongoing expenses, thus making it a potentially more cost-effective option in the long run.

Figure 4.12 Rough surface specimen scanned volume.

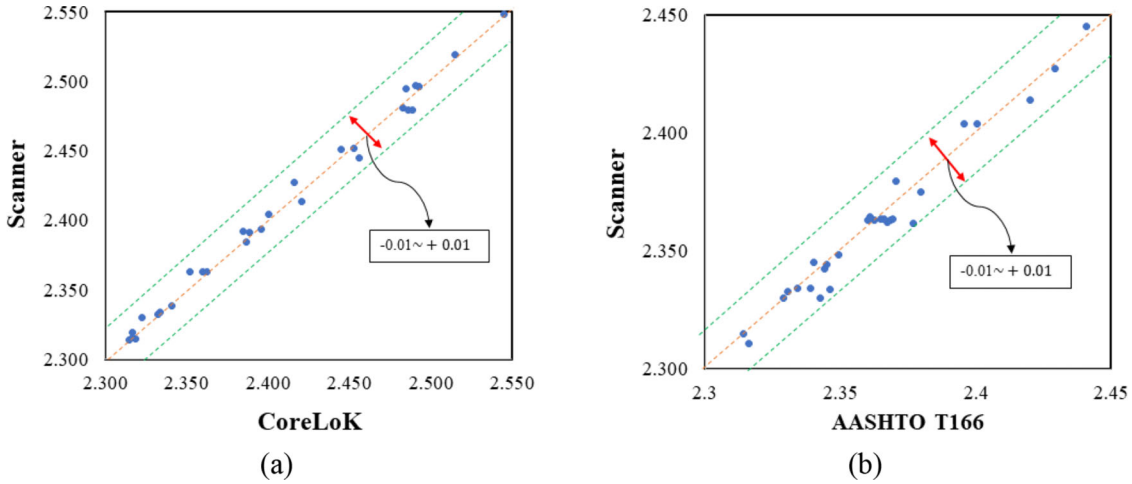

Figure 4.13 Analysis diagram: (a) scanner vs. CoreLok, and (b) scanner vs. AASHTO T166.

TABLE 4.13
Precision estimation of all G_{mb} measuring methods

Mixture Type	Fabrication Condition	Mixture's NMAS	Measurement Method		
			Scanner	AASHTO T166	CoreLok
Dense Graded Mixture	Lab-compacted	9.5	0.0003	0.0065	0.0075
		12.5	0.0018	0.0047	0.0070
		19.0	0.0006	0.0026	0.001
		25.0	0.0028	0.0060	0.0035
	Field-cored	9.5	0.0005	0.0010	0.0054
		19.0	0.0007	0.0028	0.0025
Open Grade Mixture	Lab-compacted	9.5	0.0027	N/A	0.0035
	Field-cored	19.0	0.0036	N/A	0.0054
	Lab-compacted	9.5	0.0007	N/A	0.0015
	Field-cored	19.0	0.0008	N/A	0.0030

TABLE 4.14
Equipment quote (quotes were obtained in February 2023)

Item	Equipment Cost	Additional Cost
CoreLok (InstroTek)	$8,664	Small 100 bags: $79.00 Large 100 bags: $99.00
Scanner (Afinia Pro HD)	$9,970, includes: Device: $7,699.00, Industrial Kit: $769.00 Powerful PC: $1,500	0

5. SUMMARY, CONCLUSIONS, RECOMMENDATIONS

The current techniques used to determine asphalt mixture volumetric properties have changed little since their initial adoption. However, with today's technology it is possible to measure materials properties in a more real-time format with greater accuracy. It is critical to obtain accurate bulk specific gravity (G_{mb}) measurements for compacted asphalt mixture specimens, both in the laboratory and field environments. Although some limitations of the AASHTO T166 method were resolved with the introduction of the Corelok device to measure G_{mb} of asphalt specimens, there remains some issues concerning the operation of the Corelok device. As part of the design of asphalt mixtures which are based on volumetric properties, bulk specific gravity of compacted asphalt mixtures is one of the key values used to determine the amount of air voids within the mixture. There are some limitations to the current methods, even though they have demonstrated some promising results. The AASHTO T166 method, for example, works for asphalt specimens with less than 2% water absorption. The research presented herein introduces the new imaging technique to overcome some limitations of the current available methods and to integrate them into a single method suitable for all mixture types, regardless of the mixture design, aggregate gradation, size, fabrication condition (laboratory or field cored), and surface texture. The results and analysis of this study demonstrate that introducing the imaging method into the measurement of G_{mb} of asphalt specimens has been highly successful. The following conclusion can be drawn from the current study.

- Imaging techniques can be a reliable alternative for measuring G_{mb} of any type of asphalt mixture specimen and can do so more quickly and accurately.
- There is no water absorption limitation with imaging techniques, such as the 2% limit found in AASHTO T166.
- The imaging technique is highly repeatable, when compared to CoreLok and AASHTO T166 methods.
- The accuracy of imaging techniques can eliminate the need for measurement replication.
- The proposed imaging method allows the G_{mb} measurement of asphalt mixture specimens, regardless of mixture type, aggregate size, specimen dimension, and how the specimen is obtained (laboratory produced or field cores).
- The proposed imaging method can produce a highly accurate G_{mb} measurement in 8 minutes or less.
- Measuring asphalt mixture G_{mb} by imaging does not require specific operator expertise, therefore the measurement is independent of the operator skill.

Given these conclusions, the following are recommended.

- The proposed imaging method should be further trialed in everyday use, both to collect additional data and test the equipment in less hospitable environments.
- The proposed imaging method recommends asphalt specimen G_{mb} be measured using 20 turntable steps and medium meshing level.
- To measure the G_{mb} efficiently, the scanner location should be adjusted based on the specimen dimensions, with larger specimens requiring a longer working distance between the scanner and specimen.

REFERENCES

Abdel-Bary Ebrahim, M. (2011). *3d laser scanners: History, applications, and future*. Assiut University.

Acharya, T., & Ray, A. K. (2005). *Image processing: Principles and applications*. John Wiley & Sons.

Aliha, M. R. M., Fazaeli, H., Aghajani, S., & Nejad, F. M. (2015). Effect of temperature and air void on mixed mode fracture toughness of modified asphalt mixtures. *Construction and Building Materials*, *95*, 545–555.

Amzajerdian, F., Pierrottet, D., Petway, L., Hines, G., & Roback, V. (2011). Lidar systems for precision navigation and safe landing on planetary bodies. *International Symposium on Photoelectronic Detection and Imaging 2011: Laser Sensing and Imaging; and Biological and Medical Applications of Photonics Sensing and Imaging*, *8192*, 819202.

Azari, H., Lutz, R., & Spellerberg, P. A. (2006). *Precision estimates of selected volumetric properties of HMA using absorptive aggregate*. Transportation Research Board of the National Academies.

Brown, E. R., & Cross, S. A. (1991, January). *Comparison of laboratory and field density of asphalt mixtures* (NCAT Report 91-01). National Center for Asphalt Technology (US).

Brown, E. R., Hainin, M. R., Cooley, A., & Hurley, G. (2004a). *Relationship of air voids, lift thickness, and permeability in hot mix asphalt pavements* (NCHRP Report 531). Transportation Research Board.

Brown, E. R., Hainin, M. R., Cooley, A., & Hurley, G. (2004b). *Relationships of HMA in-place air voids, lift thickness, and permeability* (Project 9–27). National Cooperative Highway Research Program.

Buchanan, M. S. (2000). An evaluation of selected methods for measuring the bulk specific gravity of compacted hot mix asphalt (HMA) mixes. *Association of Asphalt Paving Technologists Proc*, *69*, 608–634.

Cooley, L. A., Prowell, B. D., Hainin, M. R., Buchanan, M. S., & Harrington, J. (2002). *Bulk specific gravity round-robin*

using the Corelok vacuum sealing device (Report No. FHWA-IF-02-044). National Center for Asphalt Technology.

Curless, B. (1999). From range scans to 3D models. *ACM SIGGRAPH Computer Graphics*, *33*(4), 38–41.

De Freitas, E. F., Pereira, P., Picado–Santos, L., & Papagiannakis, A. T. (2005). Effect of construction quality, temperature, and rutting on initiation of top-down cracking. *Transportation Research Record*, *1929*(1), 174–182.

Dukatz, E., Haddock, J., Hall, K., Kliewer, J., Marek, C., Musselman, J., Regimand, A., West, R., Sholar, G., & Tran, N. (2009). *A review of aggregate and asphalt mixture specific gravity measurements and their impacts on asphalt mix design properties and mix acceptance* (Report 12-06). National Center for Asphalt Technology.

Edl, M., Mizerák, M., & Trojan, J. (2018). 3D laser scanners: History and applications. *Acta Simulatio-International Scientific Journal about Simulation*, *4*(4), 1–5.

Finn, F. N., & Epps, J. A. (1980, August). *Compaction of hot mix asphalt concrete* (Research Report 214-21). Texas Transportation Institute, the Texas A&M University System.

Griffith, F. T. (2009). *Investigation of the measurement of bulk specific gravity of compacted specimens by various methods*. University of Arkansas.

Hall, K. D., Griffith, F. T., & Williams, S. G. (2001). Examination of operator variability for selected methods for measuring bulk specific gravity of hot-mix asphalt concrete. *Transportation Research Record*, *1761*(1), 81–85. https://doi.org/10.3141/1761-10

Harvey, J. T., & Tsai, B.-W. (1996). Effects of asphalt content and air void content on mix fatigue and stiffness. *Transportation Research Record*, *1543*(1), 38–45.

Kassem, E., Masad, E., Lytton, R. L., & Chowdhury, A. R. (2011). Influence of air voids on mechanical properties of asphalt mixtures. *Road Materials and Pavement Design*, *12*(3), 493–524.

Kersten, T. P., Sternberg, H., & Mechelke, K. (2005). Investigations into the accuracy behaviour of the terrestrial laser scanning system Mensi GS100. *Proceeding of the Optical 3D Measurement Techniques*, *1*, 122–131.

Lee, S.-J., Amirkhanian, S. N., Putman, B. J., & Kim, K. W. (2007). Laboratory study of the effects of compaction on the volumetric and rutting properties of CRM asphalt mixtures. *Journal of Materials in Civil Engineering*, *19*(12), 1079–1089.

Liu, J., Liu, F., Zheng, C., Zhou, D., & Wang, L. (2022). Optimizing asphalt mix design through predicting effective asphalt content and absorbed asphalt content using machine learning. *Construction and Building Materials*, *325*, 126607.

Montoya, M. A., Pouranian, M. R., & Haddock, J. E. (2018). Increasing asphalt pavement density through mixture design: A field project. *Asphalt Paving Technology: Association of Asphalt Paving Technologists-Proceedings of the Technical Sessions*, 87.

Peters, W. H., & Ranson, W. F. (1982). Digital imaging techniques in experimental stress analysis. *Optical Engineering*, *21*(3), 427–431.

Saravanja, L. (2020). 3D measurement-comparison of CMM and 3D scanner. *Proceedings of the 31st DAAAM International Symposium* (pp. 0780–0787).

Schwartz, C. W., Li, R., Ceylan, H., Kim, S., & Gopalakrishnan, K. (2013). Global sensitivity analysis of mechanistic–empirical performance predictions for flexible pavements. *Transportation Research Record*, *2368*(1), 12–23. https://doi.org/10.3141/2368-02

Shen, S., Zhang, W., Shen, L., & Huang, H. (2016). A statistical based framework for predicting field cracking performance of asphalt pavements: Application to top-down cracking prediction. *Construction and Building Materials*, *116*, 226–234.

Takahashi, S., & Partl, M. N. (2001). Improvement of mix design for porous asphalt. *Road Materials and Pavement Design*, *2*(3), 283–296.

Williams, R. C., Williams, B., Kvasnak, A., Stanton, B., & Van Dam, T. (2005, October). *Development of acceptance criteria of compacted hot mixture asphalt bulk specific gravity based on vacuum sealed specimens: Volume I* (Report No. RC-1522). Michigan Technological University.

Yan, Y. (2012). *Hot mix asphalt concrete density, bulk specific gravity, and permeability* [Master's thesis, West Virginia University]. https://researchrepository.wvu.edu/etd/3348

Zeiada, W. A., Kaloush, K. E., Underwood, B. S., & Mamlouk, M. E. (2014). Improved method of considering air void and asphalt content changes on long-term performance of asphalt concrete pavements. *International Journal of Pavement Engineering*, *15*(8), 718–730.

About the Joint Transportation Research Program (JTRP)

On March 11, 1937, the Indiana Legislature passed an act which authorized the Indiana State Highway Commission to cooperate with and assist Purdue University in developing the best methods of improving and maintaining the highways of the state and the respective counties thereof. That collaborative effort was called the Joint Highway Research Project (JHRP). In 1997 the collaborative venture was renamed as the Joint Transportation Research Program (JTRP) to reflect the state and national efforts to integrate the management and operation of various transportation modes.

The first studies of JHRP were concerned with Test Road No. 1—evaluation of the weathering characteristics of stabilized materials. After World War II, the JHRP program grew substantially and was regularly producing technical reports. Over 1,600 technical reports are now available, published as part of the JHRP and subsequently JTRP collaborative venture between Purdue University and what is now the Indiana Department of Transportation.

Free online access to all reports is provided through a unique collaboration between JTRP and Purdue Libraries. These are available at http://docs.lib.purdue.edu/jtrp.

Further information about JTRP and its current research program is available at http://www.purdue.edu/jtrp.

About This Report

An open access version of this publication is available online. See the URL in the citation below.

Notani, M. A., Jahangiri, B., Rastegar, R. R., & Haddock, J. E. (2023). *Determining asphalt mixture properties using imaging techniques* (Joint Transportation Research Program Publication No. FHWA/IN/JTRP-2023/12). West Lafayette, IN: Purdue University. https://doi.org/10.5703/1288284317635